ABSTRACT

Title of Document: PORTABLE HYPERSPECTRAL IMAGING DEVICE FOR SURFACE SANITATION VERIFICATION IN THE PRODUCE INDUSTRY

Michael Sean Wiederoder, Master of Science, 2011

Directed By: Y. Martin Lo, Ph.D., Associate Professor, Department of Nutrition and Food Science

Produce processors must clean and sanitize surfaces before production to reduce the risk of foodborne illness. Current surface hygiene verification methods require direct surface sub-sampling at selected locations and a wait time. To augment these methods, a portable hyperspectral imaging device was developed to find potential contaminants in real-time and increase sub-sampling effectiveness. Analysis of hyperspectral fluorescence images showed that fresh-cut produce processing exudates in the regions of 460-540 and 670-680 nm are detectable from background materials, while select cleaning agents are not. The portable single operator imaging system includes a charge coupled device (CCD) camera, tunable optical filter, laptop, light emitting diodes (LED's) for fluorescence excitation, and a touchscreen display. Within a commercial plant, fluorescence imaging identified produce processing residuals following routine cleaning procedures that were not readily visible to the naked eye. These tests demonstrate the system's potential to enhance post-cleaning inspection, and helped improve routine cleaning procedures.

PORTABLE HYPERSPECTRAL IMAGING DEVICE FOR SURFACE SANITATION VERIFICATION IN THE PRODUCE INDUSTRY

By

Michael Sean Wiederoder

Thesis submitted to the Faculty of the Graduate School of the
University of Maryland, College Park, in partial fulfillment
of the requirements for the degree of
Master of Science
2011

Advisory Committee:
Dr. Y. Martin Lo, Chair
Dr. Alan Lefcourt
Dr. Moon Kim
Dr. Robert Buchanan

Acknowledgements

I would like to thank all my committee members for their contributions and input to the creation of this thesis. I appreciate the guidance and technical expertise of Dr. Alan Lefcourt and Dr. Moon Kim of the Environmental Microbial and Food Safety Laboratory (EMFSL) at the USDA-ARS Beltsville Agricultural Research Center (BARC). In addition, I would like to thank Dr. Robert Buchanan for providing guidance and thoughtful input on this project. I am also grateful to Dr. Y. Martin Lo for his guidance, encouragement, and direction as my major professor and thesis advisor.

I would like to express my appreciation to the staff and visiting scientists at the EMFSL (especially Diane Chan, Dr. Steve Delwiche, and Frank Gwodz for help with experiments). I also want to extend my gratitude to my fellow graduate students in Dr. Lo's group in the Department of Nutrition and Food Science: Patrick Williams, Pavan Soma, Ana Aguado, Yuting Zhou, Ansu Cherian, Melody Ge, Eirene Yossa, Sarah Yachetti, and Eric Thornber for their help and support. I wish to especially recognize Nancy Liu for her efforts in prototype construction and collection of important data.

I wish to express my thanks for the financial support of both the USDA-ARS and the University of Maryland's Department of Nutrition and Food Science and College of Agriculture and Natural Resources during this project.

Finally, I wish to thank my fiancée Dani for her love, support, and patience during the completion of this work.

Table of Contents

List of Tables

List of Figures

Chapter 1: Introduction

From 1996 to 2006, 72 foodborne illness outbreaks were associated with fresh produce consumption with 18 of these connected to fresh-cut produce (FDA 2008b). To reduce the risk of such outbreaks, produce processors clean and sanitize food contact surfaces before production starts as part of a General Hygiene Plan (GHP). A major component of the GHP includes verifying food contact surfaces are hygienic to prevent cross contamination and the potential growth of food pathogens and spoilage organisms in the processing environment.

Current industry accepted methods to monitor surface hygiene include visual inspection with the naked eye, culturing techniques, and ATP-bioluminescent assays. However, culturing techniques and ATP-bioluminescent assays require direct sub-sampling of selected surfaces, disposable reagents, and a variable wait time. These direct sample locations may not reflect real-time plant conditions and represent only limited areas of processing surfaces. A need exists for a device that can detect contaminants in real-time over a large surface area with greater sensitivity than visual inspection with the naked eye.

This study aimed at developing a portable, hyperspectral imaging system to monitor and validate surface hygiene in produce processing plants. The device should allow a processor to identify non-hygienic conditions due to known or unknown contaminants and aid in making future changes to cleaning and sanitation procedures to avoid potential food safety problems.

Chapter 2: Literature Review

Introduction

In the United States the demand for fresh fruit and vegetables continues to increase as many consumers want to improve their diet and try to follow recommendations in the USDA's 2010 Dietary Guidelines for Americans. These recommendations include increasing consumption to 2 cups of fruit and 2.5 cups of vegetables a day for a 2000 calorie diet, and eating a variety of vegetables especially dark-green, red, and orange ones (U.S. Department of Agriculture and U.S. Department of Health and Human Services 2010). From 2003 to 2008 sales of fresh fruit increased 25% to reach an estimated $24.7 billion in sales (Mintel 2009). One reason for this growth is the increase in prepared, fresh-cut fruit products that save consumers time because they are already washed, sliced, and packed for convenience (Mintel 2009). Sales of packaged salads also experienced significant growth from $2.4 billion in 2002 to $3.8 billion in 2005 before the *Escherichia coli* outbreaks in spinach caused a decline in sales in 2006 and 2007. Despite this setback, sales of packaged salads were projected to grow 2-4% per year from 2008 to 2012 in inflation-adjusted prices (Mintel 2008). The fresh-cut produce industry sold $15.9 billion of products in 2007, up from $8.9 billion in 2003, and further growth is expected (Cook 2007). Average dollar sales in grocery stores of fresh-cut or prepared vegetables increased 34.8% and sales of fresh-cut or prepared fruit increased 23.3% from 2005 to 2010 (Perishables Group 2010).

As sales continue to grow it is important to realize the possibility of an increase in foodborne illness outbreaks as more people consume produce products.

An estimated 48 million cases of foodborne illness occur annually in the United States with 29.4 percent of these illnesses deriving from produce and associated products (Scallan and others 2011; Hoffmann and others 2007). In addition, of the $152 billion in economic losses associated with acute foodborne illness annually, $39 billion is associated with fresh, processed, and canned produce (Scharff 2010).The industry's reputation and future growth relies on reducing the risk of foodborne illness associated with all produce products, including the fast growing fresh-cut sector.

Recent outbreaks of foodborne illness emphasize the need to improve produce safety. In March of 2011, cantaloupes containing *Salmonella Panama* resulted in 12 known illnesses (FDA 2011a). A recent *E. coli* O145 outbreak in May 2010 attributed to Romaine lettuce affected 5 states and caused 26 documented illnesses (CDC 2010a). In 2008, an outbreak of *Salmonella saintpaul* covered 43 states and was finally traced to Serrano and Jalapeño peppers after authorities responded to initial surveys that falsely indicated tomatoes as the primary vector (CDC 2008; Behravesh and others 2011). In 2006, an outbreak of *E. coli* O157:H7 due to bagged spinach from California affected people in 26 states, which caused a sharp drop in sales of bagged salads (Wendel and others 2009; Cook 2007). Since 2004 the FDA has confirmed the presence of *Salmonella* sp. in 28 different samples of cilantro from inside and outside the United States, which indicates a consistent problem with that product (FDA 2011b). Numerous other foodborne illness outbreaks are related to fresh and fresh-cut produce (Table 1). In general, the original source of these outbreaks was not identified until after people contracted foodborne illness.

Table 1: Recent outbreaks of foodborne illness in fresh and fresh-cut produce.

Microorganism	Product	Outbreak	Year	Reference
E. coli O157:H7	Romaine, green leaf, and butter lettuce	Recall, no reported illnesses	2007	FDA 2007
E. coli O157:H7	Spinach	199 cases	2006	Wendel and others 2009
Listeria monocytogenes	Fresh-cut Fruit (cantaloupe, honeydew, red grapes, pineapple, watermelon, or strawberry)	Recall, no reported illnesses	2006	FDA 2006
Salmonella sp.	Cantaloupe	51 cases	2008	FDA 2008a
	Cilantro	Recall, no reported illnesses	2011	FDA 2011c
Salmonella Braenderup	Tomato	82 cases	2005	Bidol and others 2007
Salmonella I 4,[5],12:i	Alfalfa Sprouts	140 cases	2011	CDC 2011
Salmonella Newport	Alfalfa Sprouts	44 cases	2010	CDC 2010b
	Tomato	115 cases	2006	Bidol and others 2007
	Tomato	72 cases	2005	Bidol and others 2007
Salmonella Oranienburg	Fruit Salad	41 cases	2006	Landry and others 2007
Salmonella Poona	Cantaloupe	155 cases	2000, 2001, 2002	CDC 2002
Salmonella Typhimurium	Tomato	190 cases	2006	Bidol and others 2007

Numerous factors increase the likelihood of pathogen contamination along the fresh and fresh-cut produce supply chain when compared to other foods. Examples include handling and mixing of large product volumes, damage of natural protection barriers, high environmental moisture and nutrient content, absence of a lethal process (e.g., heat) during production to eliminate pathogens, and possible temperature abuse during processing, storage, transport, and retail display (IFT and

FDA 2001). The produce industry attempts to prevent outbreaks from occurring by implementing practices that reduce the risk of consumers contracting foodborne illness. Surface hygiene maintenance, as a part of good hygiene practices, in produce processing plants represents one such risk reduction step.

Surface Hygiene Importance

Food contact surface contamination within a food processing plant can result in the transfer of pathogens onto finished products. In fact, an estimated 1/3 of all foodborne illness outbreaks are attributed to cross-contamination events (Gerner-Smidt and Whichard 2007). Numerous incidents of cross contamination of food products derive from improperly cleaned/sanitized equipment such as pumps, tanks, or containers used to handle raw food products (Reij and others 2004; Morgan and others 1993; Hennessy and others 1996; Llewellyn and others 1998). Direct pathogen source identification presents difficulty because many things such as soil, irrigation water, insects, inadequately composted manure, animal or human feces, and human handling can act as vectors for produce contamination (Buck and others 2003). Thus, proper hygiene to prevent cross contamination represents an important risk reduction step to prevent pathogenic bacteria from transferring to produce sold to the public. Proper surface hygiene also prevents the transfer of spoilage microorganisms that cause economic losses and poor sensory properties in produce products.

Another major concern of processors is that food environments provide ideal conditions for biofilm formation due to the presence of water, food (nutrients), soil and hard-to-clean surfaces. In fact, many clean-in-place procedures probably do not effectively remove all microorganisms, thus resulting in the potential for biofilm

formation (Kumar and Anand 1998). Bacteria cells in biofilms can release into the surrounding environment resulting in potential cross contamination events that can cause post-processing contamination and disease transmission (Poulsen 1999). Many human pathogens such as *E. coli* O157:H7, *Salmonella sp*., *Staphylococcus aureus*, and *Listeria monocytogenes* are known to attach and form biofilms on abiotic surfaces such as stainless steel, plastic, glass, and cement commonly found in food processing environments (Niemira 2007). Research also shows that *E. coil* O157:H7 in a biofilm on food contact surfaces can transfer to produce such as lettuce, carrots, cantaloupe, and spinach (Silagyi and others 2009). Of particular concern with biofilm formation, is the increased bacterial resistance to antimicrobials, UV light radiation, sanitizing agents, desiccation and oxidative stress that make them hard to clean (Donlan and Costerton 2002; Fatemi and Frank 1999). Detection of biofilm buildup and non-hygienic environmental conditions that support biofilm growth can reduce the risk of foodborne illness from produce products.

Surface Hygiene Monitoring

Industry validates surface hygiene after pre-production cleaning and sanitizing procedures to reduce the risk of pathogen contamination or microbial spoilage. An ideal hygiene monitoring technology should be capable of scanning large surfaces in a rapid, accurate, inexpensive, durable, automated, sensitive, and continuous manner to indicate unsanitary conditions that might harbor microbes. Current surface hygiene verification methods employed within industry include culturing techniques, ATP bioluminescence assays, and visual inspection with naked eye. The following paragraphs discuss these techniques and their limitations.

Sampling

Before using a culturing technique or ATP bioluminescence test, a sample must be collected from a surface of interest. Test locations are chosen based on random, representative, selective, or convenience sampling plans as part of good hygiene practices (Kvenberg and others 2000). These sampling locations include both direct contact surfaces such as pipes and conveyers and indirect surfaces such as walls and floors that can harbor hazardous microorganisms (Nivens and others 2009).

Sampling procedures to collect microbes from surfaces include either rinsing solutions or physical removal with a swab. Sterilized rinsing solutions allow sampling of large surface areas and inaccessible equipment surfaces, but often do not provide enough shear force or chemical dispersion to remove microorganisms and create large sample volumes that increase material and disposal costs (Borchert 2004). As a result, the most common sampling method utilizes a moistened, sterilized swab or sponge rubbed over a defined area before placement into a buffer solution (Borchert 2004). Advantages of direct sampling include greater ability to remove microorganisms and disadvantages include small sample area size and lack of repeatability and reproducibility due to human error (Pérez-Rodríguez and others 2008). These sampling methods require selection of a limited number of surfaces that do not necessarily reflect actual day-to-day plant operation.

Detection

The gold standard for microbiological testing is culture-counting on nutritive media to enumerate and identify the organism of interest (Banada and others 2009). Enrichment of the extracted microbes from a direct sample typically precedes

application to selective or non-selective media where, after an incubation period, the number of viable colonies are counted (Gracias and McKillip 2004). Another culturing method uses Replicate Organism Detection and Counting (RODAC) plates that contact a flat test surface with a convex agar plate that is then incubated for later enumeration (Nivens and others 2009). If desired, further analysis of a selected pure culture colony with a confirmatory assay can reveal the species present (Nivens and others 2009). One major problem with culture based methods is that only approximately 1% of all viable bacteria from an environmental sample are culturable (Maukonen and others 2003). These methods are also time consuming, labor intensive, and require at least 24-48 hours to acquire results. This lack of fast results impairs immediate response to the problem and allows production to continue when a potential problem exists.

Adenosine triphosphate (ATP) bioluminescence assays comprise a popular method to monitor surface contamination because ATP is ubiquitous in all living cells (Costa and others 2004). Within the monitoring device, luciferase and luciferin combine with ATP, collected by a specialized swab, in a magnesium buffer and emit photons that are measured with a photodetector (Lo and others 2010). The amount of light detected corresponds to the amount of ATP present (Pérez-Rodríguez and others 2008). Studies show the results of culture counting techniques, as expressed in microbial concentration, and ATPase assays, as expressed in relative light units, correspond closely on common food contact surfaces (Aycicek and others 2006). Commercial ATP bioluminescence sensors can provide results within 1 to 3 min and are not labor intensive. However, ATP testing requires direct sampling of a small

surface area, lacks specificity, cannot differentiate between live or dead cells, can miss some organic contaminants, requires a new swab for each test, and has a detection limit around 10^3-10^4 CFU/mL (Pérez-Rodríguez and others 2008).

Visual Inspection

Visual inspection with the naked eye by an employee represents an inexpensive method for companies to survey a large area of surfaces in real-time. But many contaminants that may cause problems, especially biofilms and small processing related debris that can harbor microbes, are not easily visible to the naked eye. Hyperspectral imaging, discussed in subsequent sections, maintains the advantages of visual inspection, but can detect a number of contaminants normally missed by basic visual inspection.

Hyperspectral Imaging

Fluorescence Phenomena

Fluorescence occurs when a compound absorbs light a certain wavelength and emits photons at longer wavelengths. After light absorption, electrons within a molecule reach an excited state before returning back to a ground state in approximately 10^{-12} seconds. The energy released during this step results in photon emission with less energy than the absorbed photon due to losses within the molecule (Figure 1) (Llères and others 2007). A compound's quantum efficiency measures the ratio of total energy emitted per unit of energy absorbed:

$$\Phi = \frac{number\ of\ quanta\ emittted}{number\ of\ quanta\ absorbed} = quantam\ yield\ efficiency \quad (1)$$

A Φ close to 1 indicates great observed fluorescence while a value close to zero indicates there is no measureable fluorescence for that compound.

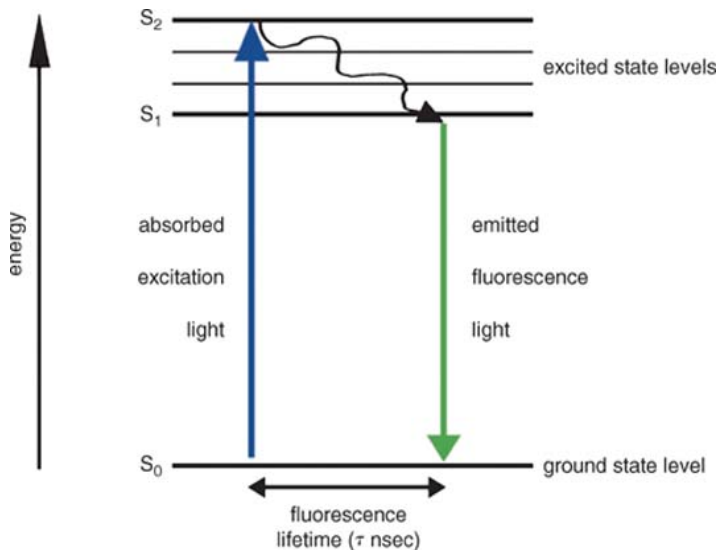

Figure 1: Jablonski diagram of Stokes shift phenomena of fluorescent compound with blue photon excitaion and green photon emission.
(source: Llères and others 2007)

Each fluorescent compound has a distinct excitation spectrum that describes the relative efficiency of radiation absorbed at different wavelengths to cause fluorescence, and a distinct emission spectrum that describes the relative intensity of the subsequent radiation emitted at different wavelengths. While the excitation wavelength can affect a compound's fluorescence emission spectrum amplitude, it generally has minimal affect on the relative shape of that same emission spectrum (Lakowicz 2006).

Stokes fluorescence is the specific phenomenon normally observed in solutions that contain fluorescent compounds (Guilbault 1990b). A physical constant called the Stokes shift describes the wavelengths of excitation and emission maxima in the following equation:

$$Stokes\ shift = 10^7 \frac{1}{\lambda_{ex}} - \frac{1}{\lambda_{em}} \quad (2)$$

where λ_{ex} and λ_{em} are the corrected maximum excitation and emission wavelength in nanometers. Figure 2 shows an example of a Stokes shift, excitation spectrum, and emission spectrum (Guilbault 1990b).

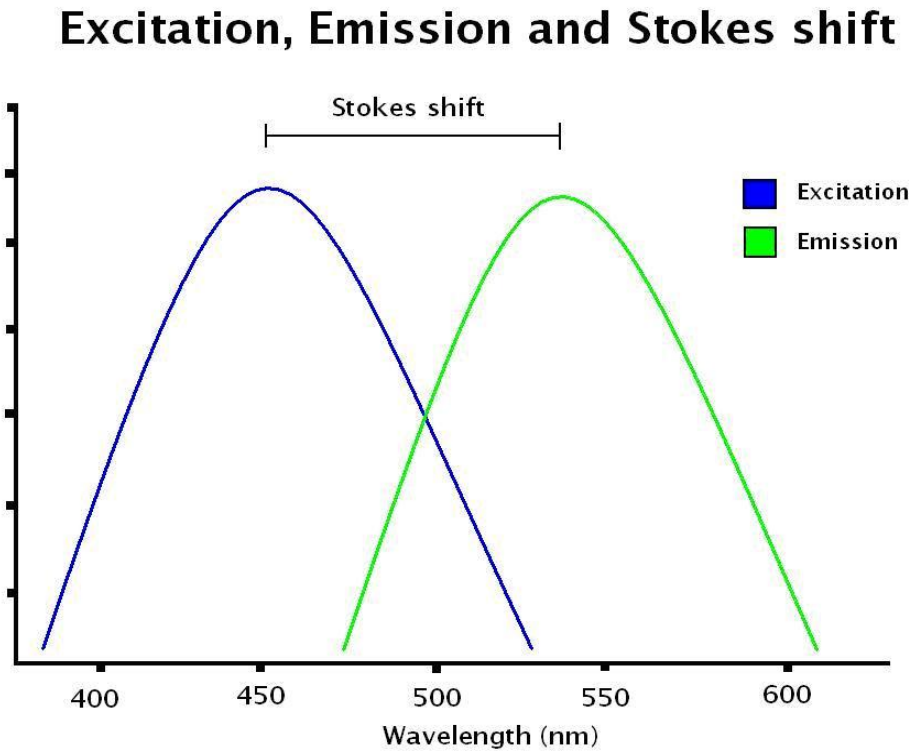

Figure 2: Example excitation and emission spectrum with Stokes shift.
(Source: Riddle 2006)

Many organic molecules fluoresce and tend to have high molar absorption of light and because of highly conjugated non-aromatic, aromatic, and heterocyclic structures (Guilbault 1990a). Chlorophyll-a, a key element in plant photosynthesis, fluoresces strongly between 670-680 nm (Brody 1958). Kok (1976) reported that chlorophyll-a in plants fluoresces at 680 nm and 740 nm bands. Chappelle and others (1991) found fluorescence bands with maxima at 420, 440, 490, and 525 nm for vitamin K, reduced nicotinamide adenine dinucleotide (NADPH), beta-carotene, and

riboflavin respectively in the blue fluorescence bands. Also lignins and other phenolics found in plant material emit blue fluorescence under ultraviolet light excitation (Fry 1979; Fry 1982; Lundquist and others 1978). These fluorescent molecules are common in produce processing residuals left behind after cleaning and sanitation, potentially making them detectable using fluorescence imaging techniques.

Factors that can affect a compound's relative fluorescence intensity include water concentration, pH, temperature, and photochemical decay. At relatively low solution concentrations there is a direct linear relationship between solution concentration and fluorescence intensity for fluorophores in water based solutions before reaching a maximum value at a higher concentration (Lakowicz 2006). When solution concentration exceeds this maximum value, the fluorescence intensity can decrease due to quenching effects. Changing the pH of a solution can alter the shape of a molecule and thus change its fluorescent properties (Wehry 1990). However, in field based experiments with water based solutions this is rarely an issue (Promega Corporation 2011). As the temperature increases the relative fluorescent intensity of solute molecules within a liquid solution decreases slightly. These temperature effects are rarely large enough to be relevant to analysis unless the solute changes shape or state due to temperature change (Wehry 1990). Photochemical decay occurs when a molecule is exposed to light, specifically ultraviolet light, and breaks down to a state where the quantum yield approaches zero, thus decreasing the material's relative fluorescence intensity.

Quenching is a phenomenon in which energy absorbed by some component of the support matrix results in less emitted photons from the excited molecule. Types of

quenching include collisional quenching, static quenching, and resonance energy transfer (Lakowicz 2006). Collisional quenching involves collisions with other molecules that cause a loss of excitation energy with common quenchers including dissolved oxygen, iodide ions, and nitroxide radicals (Guilbault 1990b). Static quenching occurs when another molecule absorbs the emitted photons from a fluorescent molecule thus lowering the signal (Lakowicz 2006). Resonance energy transfer occurs when an excited molecule transfers energy via electronic coupling to another molecule that then fluoresces and emits a photon a longer wavelength than the original excited molecule would emit (Lakowicz 2006). All of these effects can decrease the measured fluorescence intensity of a compound.

Ambient lighting can also affect the ability to detect contaminants at certain wavebands. Within produce processing plants, fluorescent lights are common due to their energy efficiency. The light emission spectrum for a fluorescent light bulb displays high intensities at certain wavelengths characteristic of metals in the light's formulation (Figure 3). Within the visible light spectrum peaks can occur near 440 nm, 490 nm, 540-550nm, and 580-610 nm depending on the light bulb formulation. Conversely troughs for these light sources can occur between 450-480 nm, 510-535 nm, 560-570 nm, and 630-710 nm. The wavebands ranges of these troughs coincide with the fluorescence emissions of previously discussed compounds, proving the potential utility of fluorescence imaging for contaminant detection.

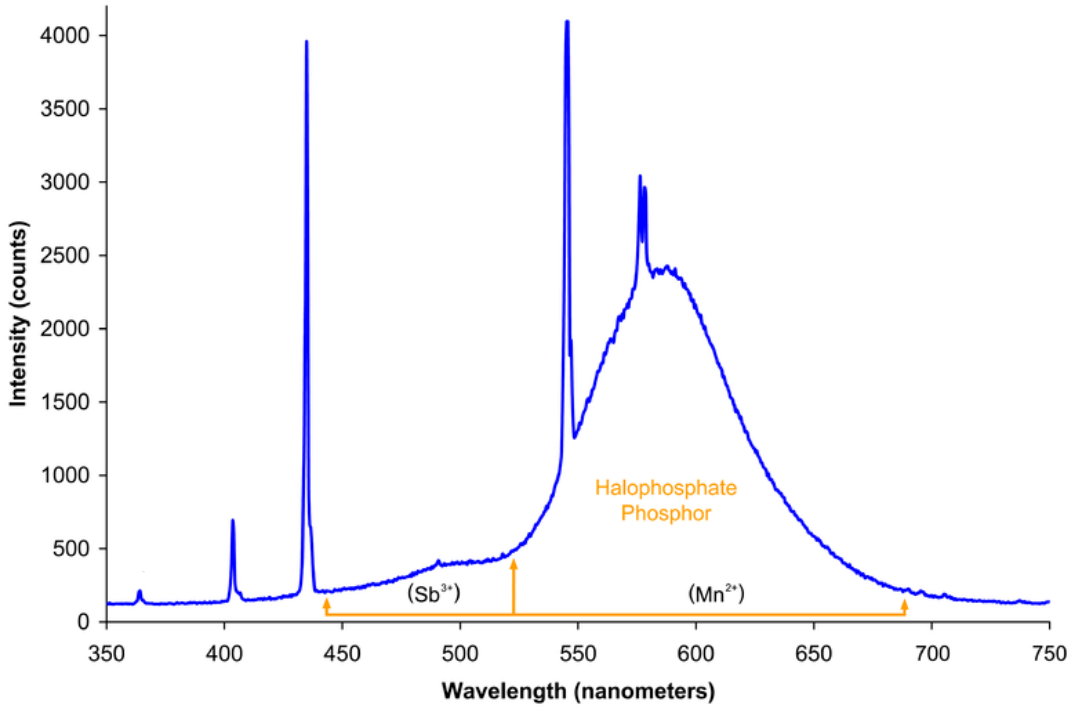

Figure 3: Electromagnetic spectrum of halophosphate type fluorescent bulb. (Source: http://en.wikipedia.org/wiki/File:Spectrum_of_halophosphate_type_fluorescent_bulb_%28f30t12_ww_rs%29.png)

Optical Detection

In the food industry optical detection is currently used mainly for sorting and evaluating quality of products. To accomplish this monochromatic or RGB-based cameras are used that relay spatial information similar to that visible to the naked eye or spectrometers are used that relay the spectral characteristics without respect to spatial orientation or location. Hyperspectral imaging combines spectroscopy measurement techniques with spatial visualization to generate a hyperspectral data cube with the three dimensions of height, width, and wavelength. As a result, hyperspectral imaging provides a great tool to assess localized defects and contaminants on commodities and food processing surfaces (Kim and others 2001).

Hyperspectral cube acquisition requires use of either a band sequential method or a line-scan method. The band sequential method integrates a series of two dimensional images captured at different individual wavelengths to generate a hyperspectral cube. The line-scan or "push-broom" method images an object one line of pixels at a time while the object moves transversely across a camera's field of view. This method concatenates the sequential line scan images to create a hyperspectral data cube. The line-scan method works optimally for conveyors and moving scanners, while a band sequential method works optimally for imaging static objects. Numerous hyperspectral imaging studies identified a few relevant wavelengths for simpler image processing methods to rapidly inspect food products and therefore increase processing speed (Kim and others 2002; Kim 2002; Mehl and others 2002; Park 2002; Qin and others 2008). Development of these simpler methods allows for the potential commercial implementation of multispectral imaging with more cost-effective instrumentation.

Hyperspectral data cube collection can be generated with reflectance or fluorescence imaging. Reflectance uses a white light source, often ambient, to illuminate an object that reflects back light with different intensities at different wavelengths. Fluorescence detection requires a light source at a characteristic wavelength, often ultraviolet (UV), which causes a target substance to emit photons at distinct, longer wavelengths. Depending on application, each method constitutes a potentially useful method for visual analysis.

Numerous hyperspectral imaging studies have demonstrated methods to detect defects associated with produce as well as potentially harmful contaminants that can

lead to increased pathogen risk. Examples of whole produce inspection include canker on citrus fruits (Qin and others 2008), fungal spores on tomatoes (Hahn and others 2004), apple defects (Mehl and others 2004; Ariana and others 2006; Lee and others 2008), apple bruises (Xing and De Baerdemaeker 2005), and even walnut shell sorting (Jiang 2007). Previous studies show fluorescence detection of fecal material, a significant potential pathogen vector, on apples (Kim 2002), strawberries, and cantaloupe (Vargas and others 2005). Fluorescence imaging is more sensitive than reflectance imaging for detection of diluted or thin smear fecal contamination on apples (Kim 2002; Liu and others 2007). Evidence of fecal contamination on an apple is still detectable when the fecal material either dries and flakes off (Kim and others 2005) or the apple is washed and brushed (Lefcourt and others 2003). The optimal wavelength for detection of fluorescent emission of feces on apples is 670 nm with two band ratios of 670 to 450 or 550 nm providing improved sensitivity (Kim and others 2005). The ability to detect fecal contamination and chlorophyll-a containing plant debris enhances the potential for hygiene inspection as both of these materials should not remain on surfaces after cleaning and sanitation.

Numerous studies of multispectral imaging in the food industry show the potential for a portable imaging system. Previous studies show the detection of poultry feces (Kim and others 2003) and other contaminants such as fat and digestive tract contents in processing plant conditions (Kim and others 2006; Cho and others 2007; Cho and others 2009). These studies resulted in the development of a handheld inspection device being commercialized for the poultry industry with one excitation wavelength and one detection wavelength. Other studies prove that hyperspectral

imaging based on fluorescence can detect biofilm build-up on common food processing surfaces such as stainless steel, high density polyethylene, plastic laminate (Formica), and two types of polished granite (Jun and others 2009; Jun and others 2010). These monoculture biofilms of *Salmonella* and *E. coli* O157:H7, grown in M9C media on the aforementioned surfaces, fluoresce with maximum emission intensity at 480 nm. The ability to detect a biofilm would allow a company to initiate proper cleaning and sanitation procedures to remove the hazard.

Whitehead and others (2008) used ultraviolet light excitation for fluorescence based detection of meat (beef), fish, and cheese exudates at various concentrations on stainless steel, and correlated findings with ATP bioluminescence testing. Results demonstrated the ability to detect solutions containing fish protein, casein, bovine serum albumin, cholesterol, fish oil, fatty acids, glycogen, starch, and lactose at various concentrations on stainless steel with an epifluorescent microscope that had wide bandpass filters (330-380 nm, 510-560 nm, and 590-650 nm) (Whitehead and others 2008). While all the exudates were detectable at a concentration of 0.1%, only the meat exudate at 10% concentration registered a positive ATP bioluminescence test. However, after pathogen inoculation each exudate yielded a positive ATP bioluminescence test result while there is no detectable difference in fluorescence response. Fluorescence imaging may not identify the build-up of harmful pathogens in meat exudates, but it can show the presence and location of the exudates before any microbes grow in it, unlike an ATP bioluminescent test. A fluorescence imaging system may detect surface contamination before other currently used methods and

allow a produce processor to remove potential contaminants before microorganisms use them to survive and grow.

Summary

A hyperspectral imaging system has the potential to improve hygiene verification efficacy to reduce the risk of produce related foodborne illness outbreaks and product spoilage. Current surface monitoring methods require direct surface sub-sampling leaves that may miss potential contaminants and a variable wait time. However, an imaging device that gathers information in real-time, indirectly (no sample destruction), over large surface areas, and without disposable reagents would allow a produce processor to immediately address potential hazards. Construction of a potable hyperspectral imaging system for background research could provide critical information for development of a cost-effective imaging device for industry.

Chapter 3: Research Goals & Objectives

The project goal is to improve surface hygiene verification by developing a portable hyperspectral imaging device to detect contaminants left behind after pre-production cleaning and sanitation procedures in produce processing facilities. Such a device can serve as the basis for development of a cost-effective commercial device for the produce processing industry. Completion of the following objectives will result in achievement of this goal:

Objective 1: Conduct spectral characterization substances expected in produce processing facilities including:

a) Sanitizers and cleaners such as CleanEdge 3022, CleanEdge 6911, sodium hypochlorite solution, and Tsunami 200
b) Produce processing residuals such as cantaloupe, honeydew, pineapple, green pepper, and watermelon exudates and leafy green, carrot, and celery wash water solutions

Objective 2: Develop and optimize a portable hyperspectral imaging device to examine surface hygiene in produce processing plants

Objective 3: Test device in a commercial facility to determine relevant wavelengths for contaminant detection and to explore for previously undiscovered contaminants

Chapter 4: Spectral Characterization of Background Substances

Introduction

This chapter examines the feasibility of using hyperspectral imaging to detect known potential contaminants in produce processing plants after cleaning and sanitation procedures. Test substances imaged included potential contaminants that could support unwanted microbial growth, such as fresh-cut produce processing exudates, and select wash waters, cleaners, and sanitizers found in industry. Hyperspectral characterization is done with a laboratory imaging system to minimize spectral artifacts caused by lighting in industrial processing plants and achieve best results. The spectral information generated facilitates development of a commercially viable portable imaging system by identifying relevant wavelengths to detect unwanted processing residuals, and not cleaners or sanitizers on processing surfaces. No known study exists that characterizes the fluorescence spectrums of these substances.

Materials and Methods

The fluorescence emission spectra of fresh-cut cantaloupe exudates and dilutions of these exudates created in-house were generated to identify wavelengths where they were detectable from background. Cantaloupe was of particular interest because of its association with numerous foodborne illness outbreaks. Similar tests were done with select cleaners and sanitizers to determine if these compounds commonly found in processing environments are detectable from background surfaces. Finally, select fresh-cut produce processing exudates collected from

industry were analyzed to determine wavebands at which they are detectable with fluorescence imaging.

A laboratory based line-scan hyperspectral imaging device (Figure 4) with ultraviolet light excitation was utilized to determine the fluorescence spectra, as measured in relative fluorescence intensity (RFI), of the test solutions on high density polyethylene (HDPE) and stainless steel surfaces common in food processing facilities. A spectrometer was not used in this study because the intended application of this research is to determine feasibility of surface contaminant detection with spatial imaging methods.

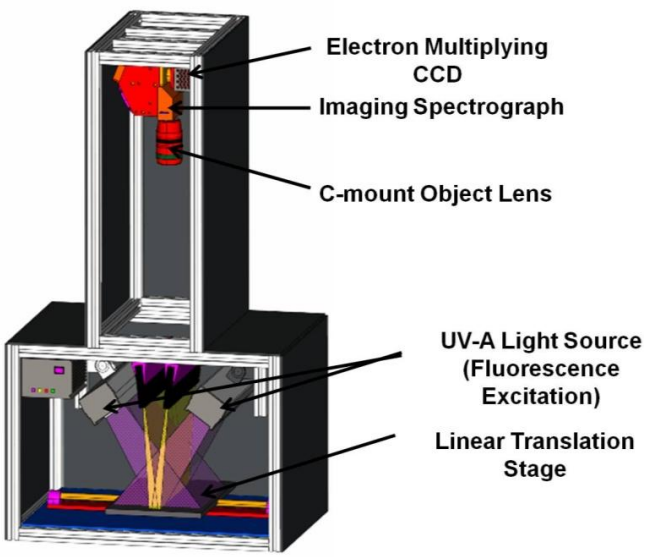

Figure 4: Laboratory based hyperspectral fluorescence system.

Samples Tested

Fresh cut cantaloupe exudates were prepared in laboratory to simulate exudates found on cutting boards in a commercial processing facility. Western cantaloupes purchased from local grocery stores were submerged in a 100 ppm free chlorine solution and cut on a high-density polyethylene cutting board. The top and bottom portion of the cantaloupe was removed with medial cuts and discarded. Next

the remaining rind was removed with vertical cuts and discarded. After cutting the melon in half with a longitudinal slice, the seeds and pulp within the seed cavity were manually removed with a scoop. The remaining hemispheres of the cantaloupe were cut into 2-3 cm slices and chopped into 1-2 cm wide pieces similar to a previous study (Fan and others 2009). The cantaloupe pieces were removed from the board by hand and the remaining exudate was collected with a disposable pipet. Serial dilutions of select exudates were prepared at ratios of 1-10, 1-20, 1-40, 1-80, and 1-160 in distilled water to allow sensitivity testing.

Cleaning and sanitation solutions analyzed (Table 2) were diluted in distilled water to the manufacturer's recommended concentration for use. These solutions are ubiquitous in processing environments as many sanitizers are left on food contact surfaces. As such they represent an important possible background signal that could reduce the effectiveness of imaging techniques.

Table 2: Select cleaners and sanitizers collected for hyperspectral study.

Cleaner or Sanitizer	Manufacturer	Description
CleanEdge 3022	CleanEdge, Baltimore, MD	sodium hydroxide and sodium hypochlorite based cleaner
CleanEdge 6911	CleanEdge, Baltimore, MD	industrial degreaser
Sodium hypochlorite	Clorox, Oakland, CA	sodium hydroxide sanitizer
Tsunami 200	Ecolab, St. Paul, MN	acid based sanitizer

Select processing exudates were obtained during commercial production at a commercial produce processing facility denoted as Company A. Exudates were collected from cutting boards for fresh-cut green peppers, pineapple, honeydew, cantaloupe, oranges, and watermelon with a disposable pipet. Wash water from fresh-cut processing of celery, carrots, and leafy greens was also collected.

All produce exudates were characterized by measuring their pH, soluble solids content, and total solids content. The pH was measured three times with a pH probe (AB15, Fisher Scientific, Pittsburgh, PA) and averaged. The soluble solids content (°Brix) was measured with a hand refractometer (AO 10431, Scientific Instruments, Keene, NH) two times and averaged. The total solids content was measured using a standardized drying method (AOAC 44.1.03 B).

Sample Preparation

Background surface materials used include stainless steel and high density polyethylene (HDPE) due to their prevalence in the produce processing industry. Coupons measuring 10.24 x 10.24 cm were washed with soap, rinsed once with SaniHol 70 (Decon Laboratories, Inc., King of Prussia, PA) and distilled water, and dried. Three 100 uL droplets of each test solution were dispensed onto coupons in a row parallel to the image scanning direction. This technique minimized spectral effects caused by uneven light distribution in the imaging set-up.

Hyperspectral Fluorescence Imaging System

The laboratory hyperspectral system utilized for this study (Figure 4) consists of an electron-multiplying charge-coupled-device (EMCCD; MegaLuca R, ANDOR Technology, South Windsor, CT), an imaging spectrograph (VNIR Concentric Imaging Spectrograph, Headwall Photonics, Fitchburg, MA), a C-mount object lens (F1.9 35 mm compact lens, Schneider Optics, Hauppauge, NY), and two UV-A lamps (EN-280 L/12, Spectronics Corp., Westbury, NY) for fluorescent excitation. Samples collected from the commercial processing facility were imaged with light balancing

filters, two cooling filters (Kodak Wratten 82C, Eastman Kodak Company, Rochester, NY, USA) and one ultra violet adsorbing filter (Kodak Wratten 2A) to dampen red fluorescence intensity and amplify blue-green fluorescence intensity.

In-house interface software developed using Microsoft Visual Basic (version 6.0, Microsoft, Seattle, WA) facilitated imaging system control, data acquisition, and image processing and analysis. Vertical pixels (spectral) were binned by 6 resulting in 60 distinct spectral bands between 421 nm and 702 nm in approximately 4.7 nm intervals. Horizontal pixels were binned by 2 (= 502 pixels) to result in a spatial resolution of approximately 0.25 mm. A motorized positioning table held two sample plates and moved them across the linear field of view in 0.25 mm increments during scanning, using a push-broom imaging approach. Dark current subtraction was completed on all hyperspectral data before image processing using a dark reference standard collected without UV illumination with similar gain and exposure time conditions. A relatively high gain (50-100) was used to allow for a short exposure time that minimized sample drying when imaging the large sample surface area. More details of the hyperspectral system are available in a previous study (Jun and others 2009).

Image Analysis

In-house software developed using Microsoft Windows Visual Basic (Version 6.0) calculated the average light intensity of an area measuring 54-66 pixels in the center of each test droplet. The average relative fluorescence intensity (RFI) values for all three test droplets was generated at wavebands between 421 and 702 nm in 4.7 nm intervals and averaged. To smooth data and reduce signal noise effects caused by

imaging at high gains with a short exposure time, a simple moving average was calculated between 430.5 and 692.3 nm with the equation:

$$RFI_{ave@\lambda n} = \frac{RFI_{(\lambda n-9.5nm)}+RFI_{(\lambda n-4.7nm)}+RFI_{(\lambda n)}+RFI_{(\lambda n+4.7nm)}+RFI_{(\lambda n+9.5nm)}}{5} \quad (1)$$

where RFI = relative fluorescence intensity (unitless) and $\boldsymbol{\lambda}$n = wavelength (nm). The RFI_{ave} for each solution between 430.5 and 692.3 nm was then graphed using Excel (2007, Microsoft, Seattle, WA). These graphs were visually inspected to identify wavebands at which relative fluorescent intensity peaks occurred or the amplitude exceeded that of the background substrate.

Results

These experiments show what test substances are detectable from background substrates with fluorescence imaging at specific wavelengths. Substances examined included fresh cut produce exudates, wash waters, sanitizers, and cleaners. Results are discussed in terms of relative fluorescence intensity (RFI).

Hyperspectral Fluorescence Imaging of Fresh-cut Cantaloupe Exudates

The fluorescence spectra of cantaloupe exudate droplets (Table 3) on high density polyethylene (HDPE) and stainless steel (SS) illuminated with ultraviolet-A light for fluorescence excitation was collected (Figures 5 and 6). At all wavebands the measured average RFI for each cantaloupe solution exceeded the background material and distilled water. Two major RFI peaks occurred at wavelengths of 459.1 nm and 682.8 nm regardless of background material with some minor peaks at 482.9, 535.2, and 540 nm. The RFI trough occurred at 649.5 nm on both background substrates. While wavebands where these peaks and troughs occur were similar, each cantaloupe

displayed a different RFI amplitude over the spectrum range. The higher the total or soluble solids content, the greater each exudate's RFI from 430.5 to 563.8 nm. However, the total or soluble solids content did not correlate with the amplitude of the RFI from 670 to 692.3 nm. Potential variability sources might include signal noise, ROI selection, lighting effects, and cantaloupe ripeness when cut.

Table 3: The pH, soluble solids (°Brix), and total solids content of three fresh-cut cantaloupe exudates prepared in the laboratory.

Cantaloupe	pH	Soluble Solids (°Brix)	Total Solids (%)
A	7.50	7.75	7.710
B	7.57	8.38	8.344
C	7.61	8.63	8.339

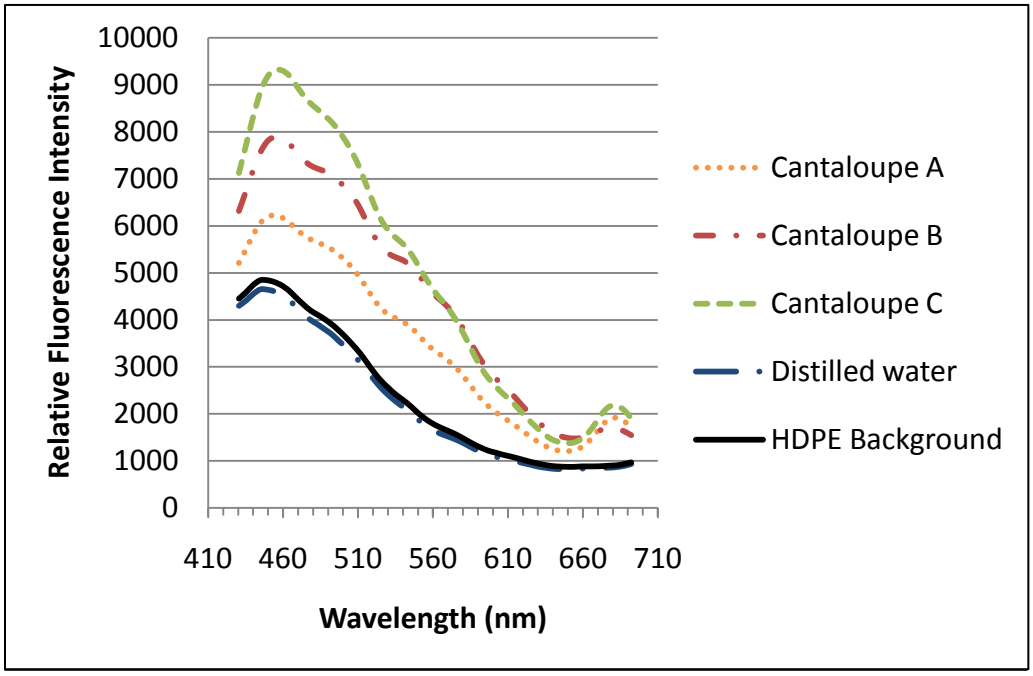

Figure 5: Representative fluorescence spectra of fresh-cut cantaloupe exudates and distilled water droplets on HDPE from 430.5 to 692.3 nm.

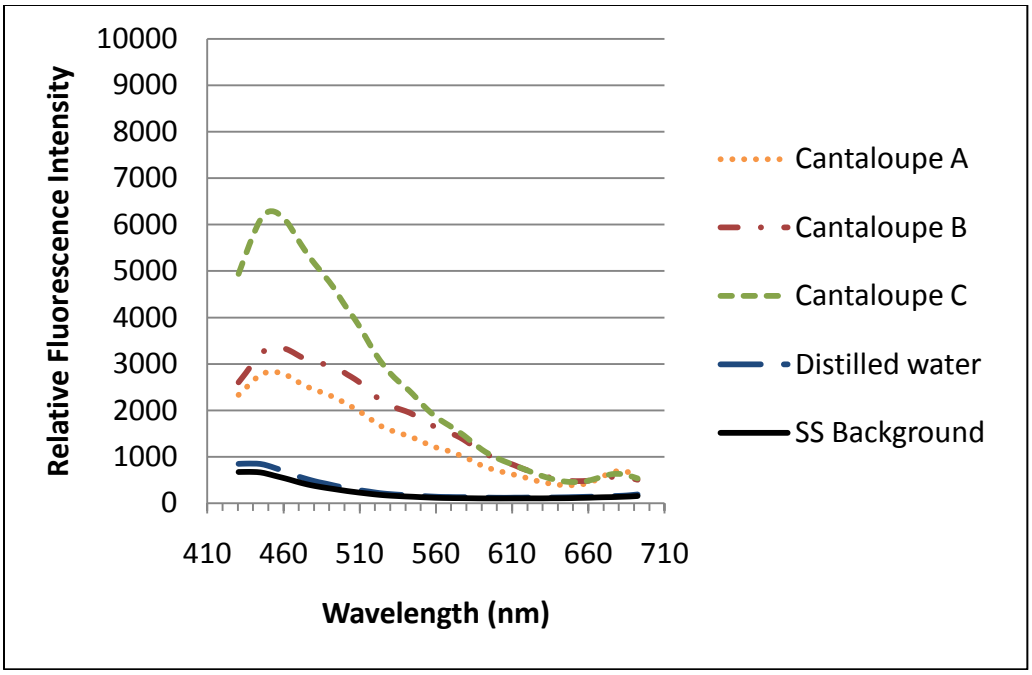

Figure 6: Representative fluorescence spectra of fresh-cut cantaloupe exudates and distilled water droplets on stainless steel (SS) from 430.5 to 692.3 nm.

The white HDPE background fluoresced under UV excitement with RFI peaks between 435.3 and 482.9 nm and troughs between 639.9 and 682.8 nm. In contrast, distilled water had no unique peaks or troughs on either background from 430.5 to 692.3 nm. The stainless steel did not fluorescence over the spectrum analyzed with a peak RFI at 435.3 nm likely due to excitation source spill. RFI amplitude for each exudate was greater on HDPE than stainless steel because of background flourescence, while the wavelength range of detectability was independent of background material.

The RFI of dried cantaloupe exudates was also measured (Figures 7 and 8). The RFI amplitude of each exudate increased over the spectrum examined after drying and the waveband range of detectability remained the same. As expected, when water evaporated the solution concentration increased, causing an increase in RFI amplitude likely due to less fluorescent signal quenching by water.

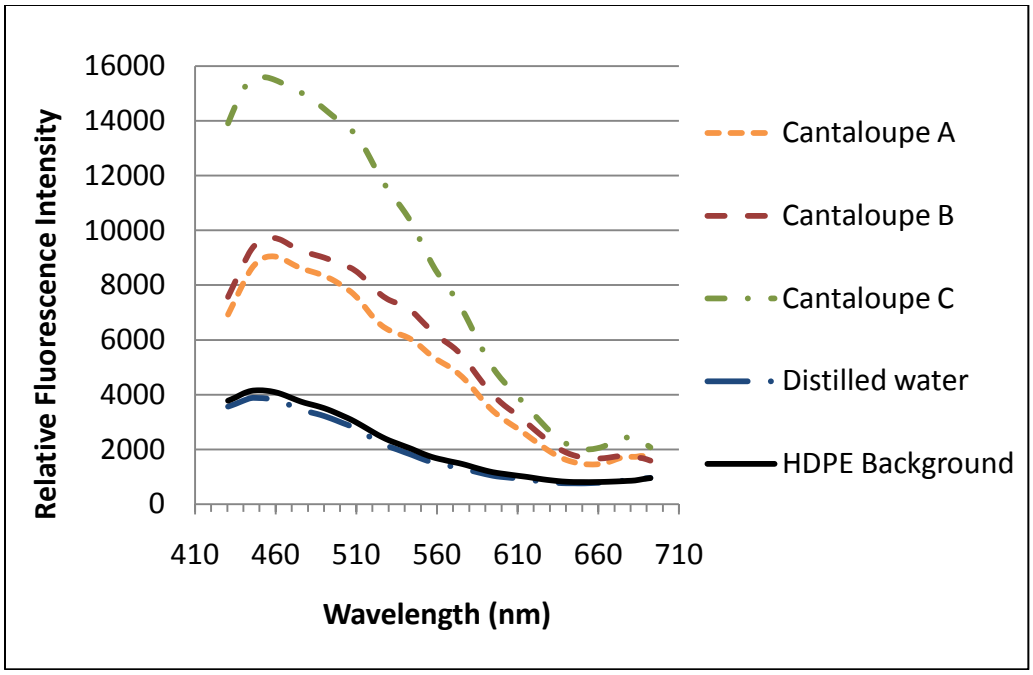

Figure 7: Representative fluorescence spectra of dried fresh-cut cantaloupe exudates and distilled water droplets on HDPE from 430.5 to 692.3 nm.

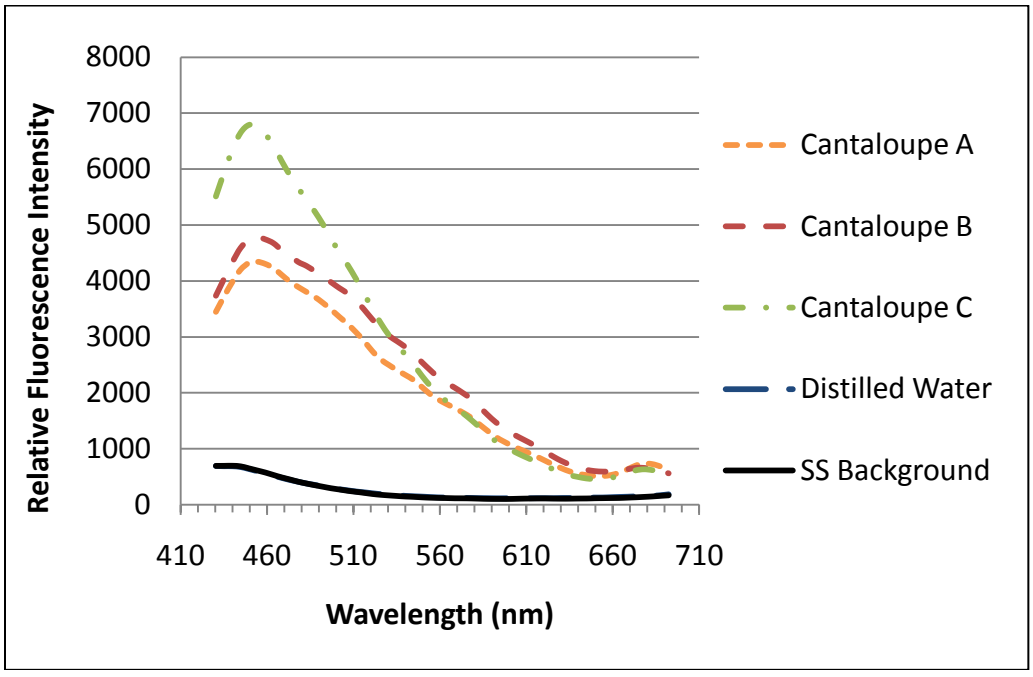

Figure 8: Representative fluorescence spectra of dried fresh-cut cantaloupe exudates and distilled water droplets on stainless steel from 430.5 to 692.3 nm.

The fluorescence spectra of a Western cantaloupe exudate (Table 4) and subsequent dilutions was collected similar to previous samples (Figures 9 and 10). When the exudate was diluted the RFI amplitude decreased as concentration decreased while an emission peak still existed at 682 nm. The lowest detectable dilution from background substrate was 1-80 on stainless steel and 1-40 on HDPE using the 682 nm waveband. With wavebands between 460 and 630 nm the lowest detectable dilution was 1-80 on stainless steel and 1-10 on HDPE due to high background fluorescence. However, when the solutions dried the lowest detectable dilution with this technique increased (Figures 11 and 12). After drying, the lowest detectable dilution was 1-80 on both stainless steel and HDPE from 460-500 nm and 1-160 on HDPE and 1-80 on stainless steel from 670-700 nm. Dilutions previously undetectable on the HDPE background now had higher RFI from 460-500 nm allowing detection. The stainless steel background displayed a peak near 520 nm likely due to capturing of some background signal at the high gain settings.

Table 4: The pH, soluble solids (°Brix) and total solids content of western cantaloupe exudate used in dilution detection trials

pH	Soluble Solids (°Brix)	Total Solids (%)
7.83	9.00	8.299

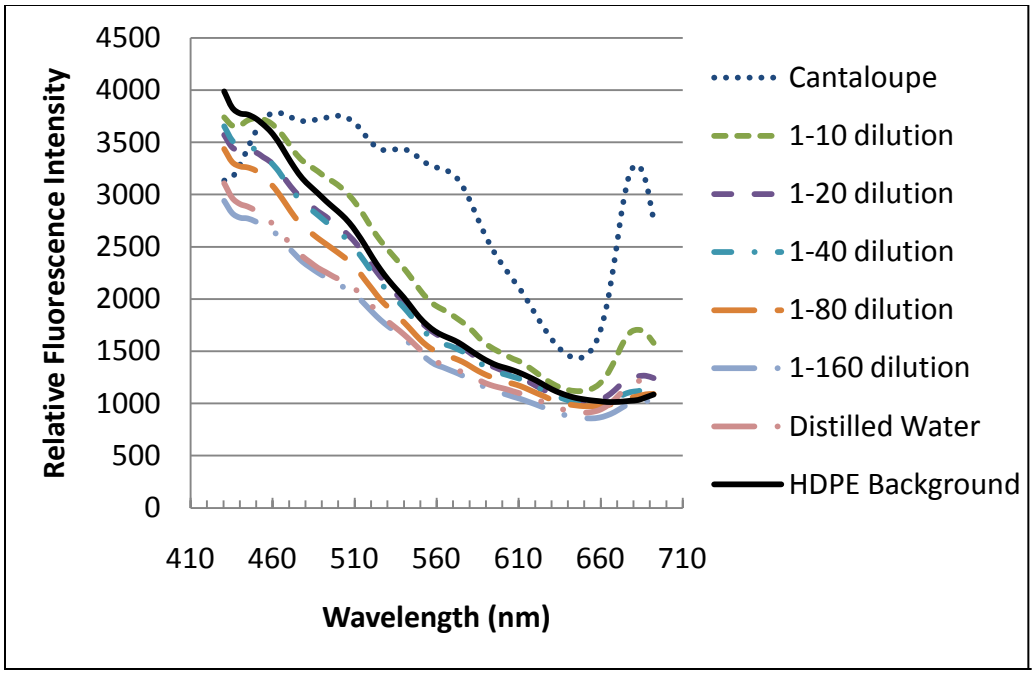

Figure 9: Representative fluorescence spectra of dilutions of a fresh-cut cantaloupe exudate on HDPE between 430.5 to 692.3 nm.

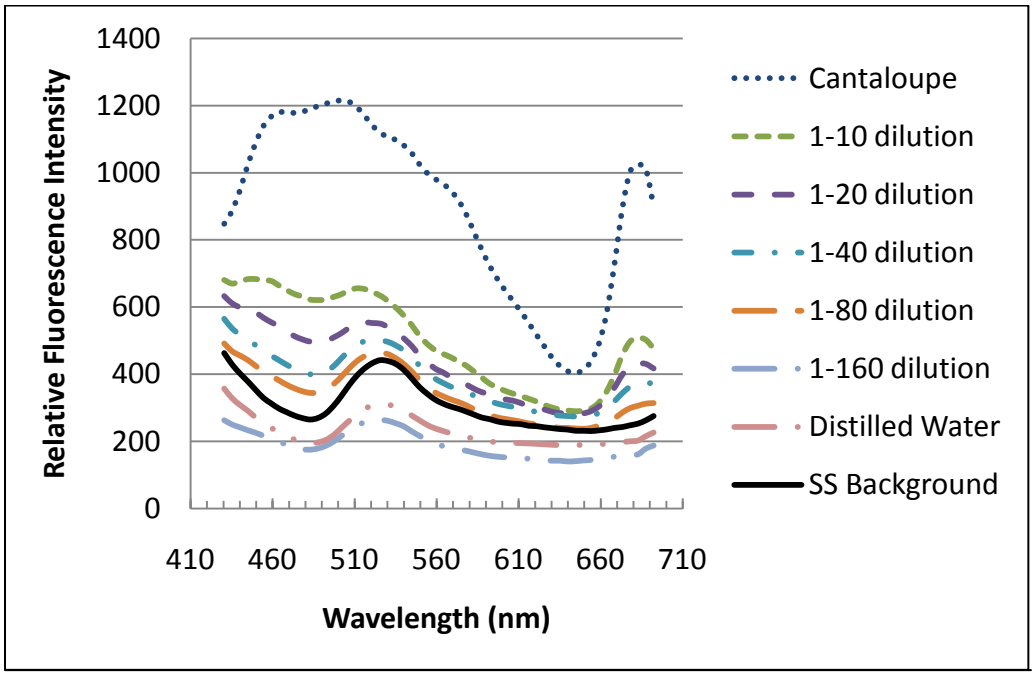

Figure 10: Representative fluorescence spectra of fresh-cut cantaloupe droplets with various dilutions on stainless steel from 430.5 to 692.3 nm.

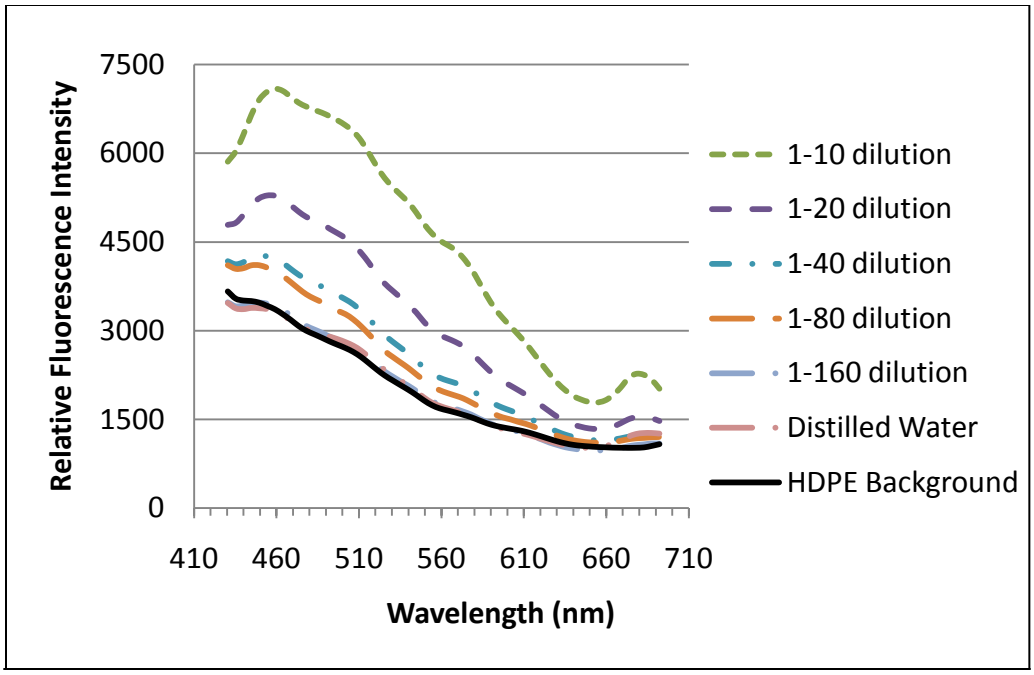

Figure 11: Representative fluorescence spectra of fresh-cut cantaloupe droplets with various dilutions on HDPE from 430.5 to 692.3 nm after 4 hours drying.

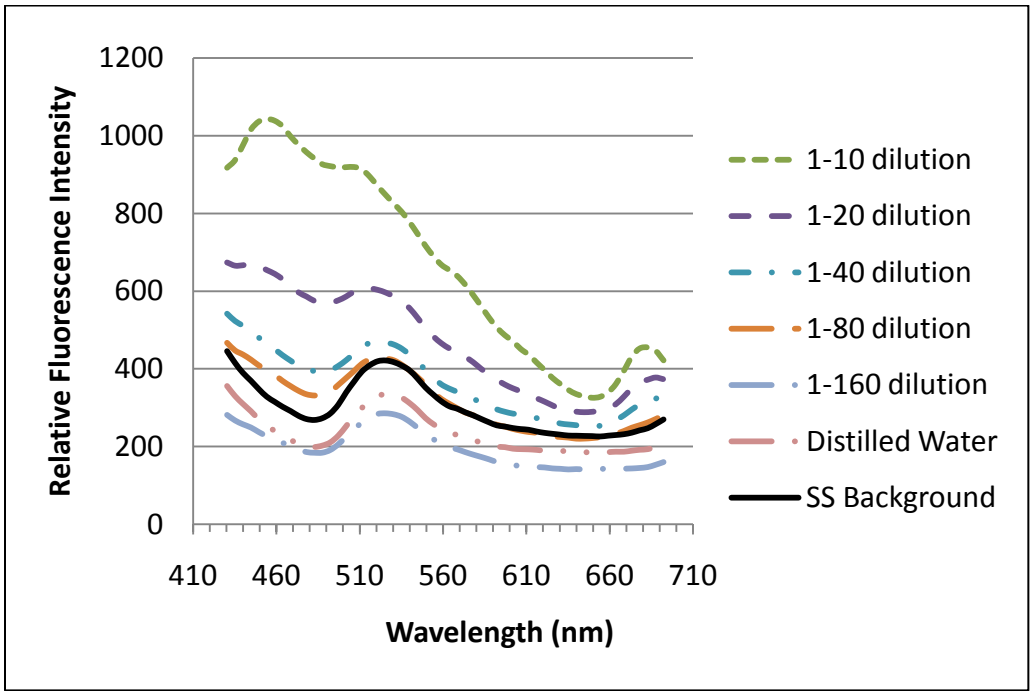

Figure 12: Representative fluorescence spectra of fresh-cut cantaloupe dilution droplets on stainless steel from 430.5 to 692.3 nm after 4 hours drying.

Hyperspectral Fluorescence Imaging of Cleaners and Sanitizers

The fluorescence emission spectra of CleanEdge 6911, chlorine solution, CleanEdge 3022, Tsunami 200, distilled water, HDPE, and stainless steel was collected before (Figures 13 and 14) or after drying (Figures 15 and 16). The solutions investigated were not detectable from background HDPE or stainless steel at any wavelength examined before and after drying. The RFI amplitude did not exceed background and there are no distinct peaks or troughs between 430.5 and 701 nm. Slight differences in RFI amplitudes are probably attributed to lighting inconsistencies, signal noise, droplet conformation, or other factors.

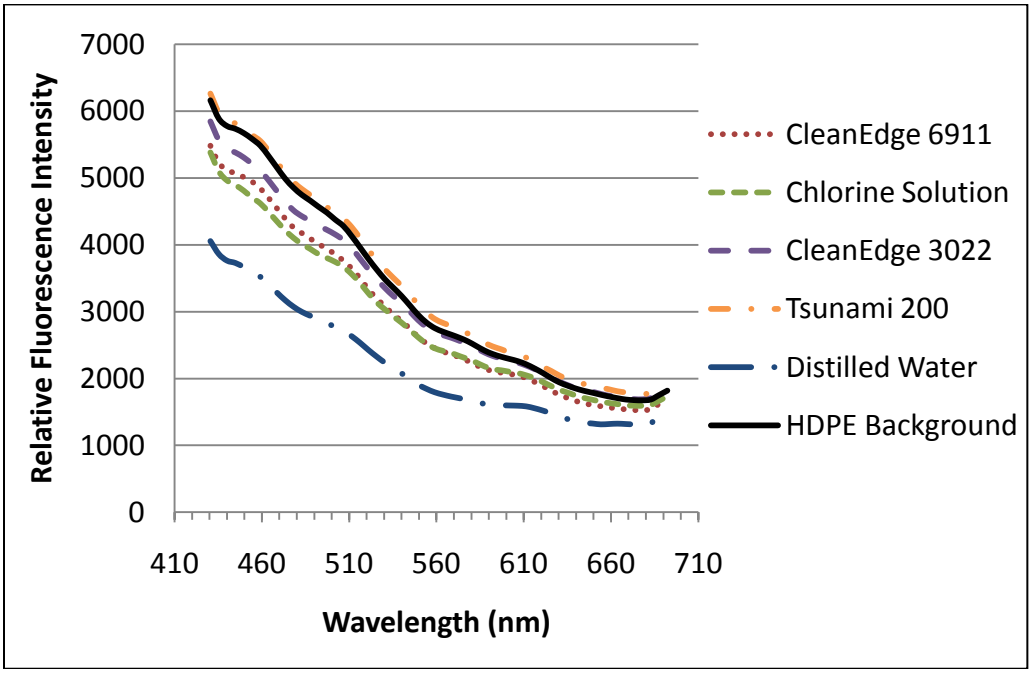

Figure 13: Representative fluorescence spectra of selected cleaners and sanitizers on HDPE from 430.5 to 692.3 nm.

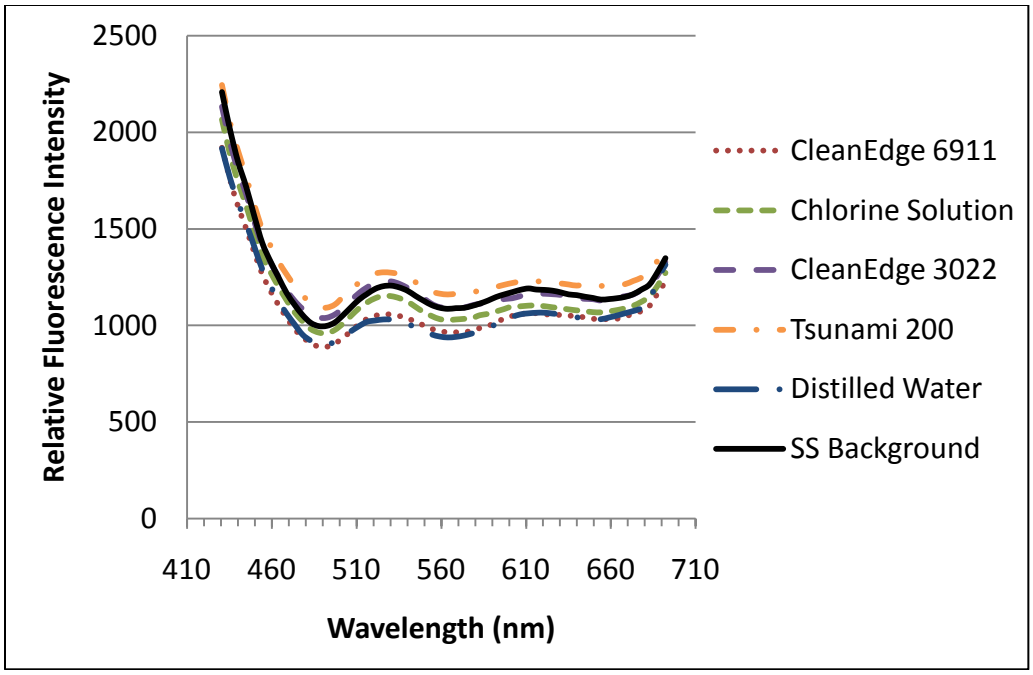

Figure 14: Representative fluorescence spectra of selected cleaners and sanitizers on stainless steel (SS) from 430.5 to 692.3 nm.

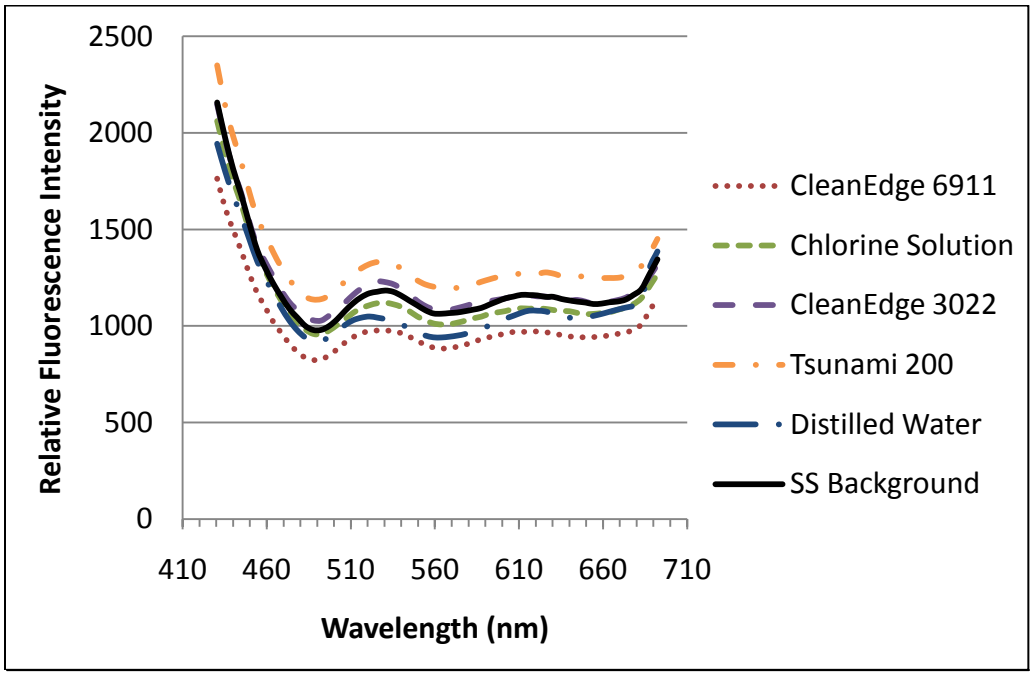

Figure 15: Representative fluorescence spectra of fully dried selected cleaners and sanitizers on stainless steel from 430.5 to 692.3 nm.

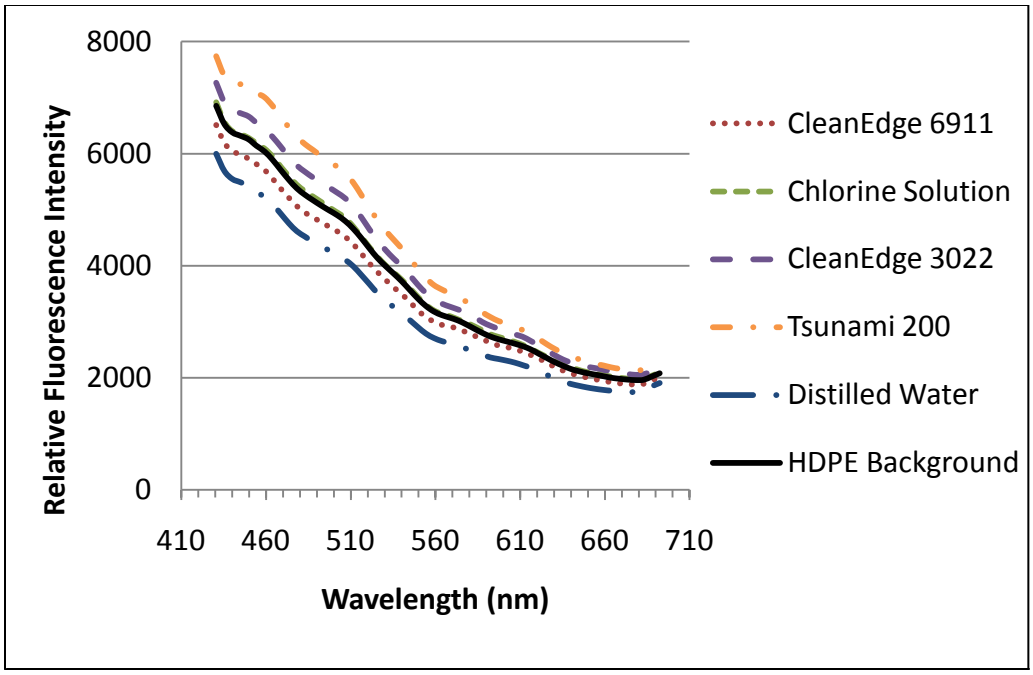

Figure 16: Representative fluorescence spectra of fully dried selected cleaners and sanitizers on HDPE from 430.5 to 692.3 nm.

Hyperspectral Fluorescence Imaging Produce Processing Samples

From Company A, samples of select fresh-cut produce processing exudates and wash waters were collected during production. The pH, soluble solids content (°Brix), and total solids content (mass solids/mass solution) of each sample was analyzed to understand the properties of each test solution from two separate visits termed Trial 1 (Table 5) and Trial 2 (Table 6). The fluorescence emission spectra of these industry samples were collected from 430.5 to 692.3 nm under UV illumination on HDPE for Trial 1 (Figures 17 and 18) and stainless steel for Trial 2 (Figure 19). Some signal noise was caused by the filters used because they are intended for perpendicular light and cause non-uniform light effects when the angle of incident light is not 90 degrees.

Table 5: The pH, soluble solids (°Brix) and total solids content of selected processing exudates imaged in Trial 1.

Solution	pH	Soluble Solids (°Brix)	Total Solids (%)
Cantaloupe	7.20	10.5	9.316
Carrot wash water	6.40	0	0.000
Green pepper	5.52	0.5	0.776
Honeydew	6.42	8.75	7.950
Leafy green wash water	6.54	0	0.000
Pineapple	3.43	7.5	6.797
Watermelon	5.83	9.5	9.433

Table 6: The pH, soluble solids (°Brix) and total solids content of selected processing exudates imaged in Trial 2.

Solution	pH	Soluble Solids (°Brix)	Total Solids (%)
Cantaloupe	6.37	7.5	7.382
Carrot Wash Water	6.56	0	0.108
Celery Wash Water	6.70	0	0.000
Honeydew	6.79	9.25	9.086
Pineapple	3.45	10.75	10.438
Orange	4.09	13.5	12.543

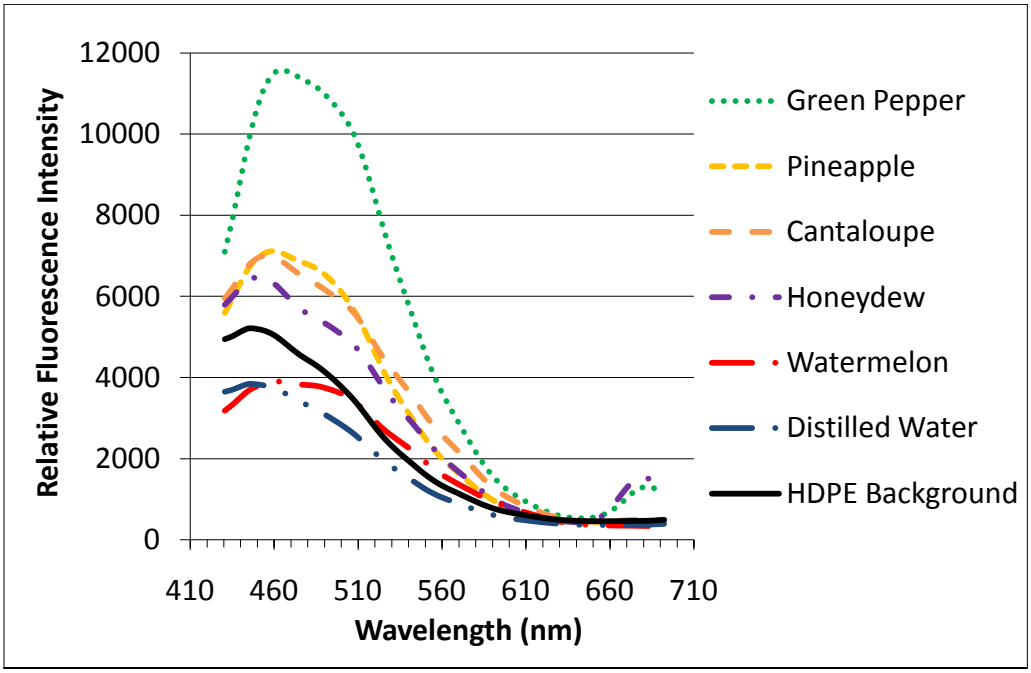

Figure 17: Representative fluorescence spectra of various fresh-cut produce processing exudates from Trial 1 on HDPE from 430.5 to 692.3 nm.

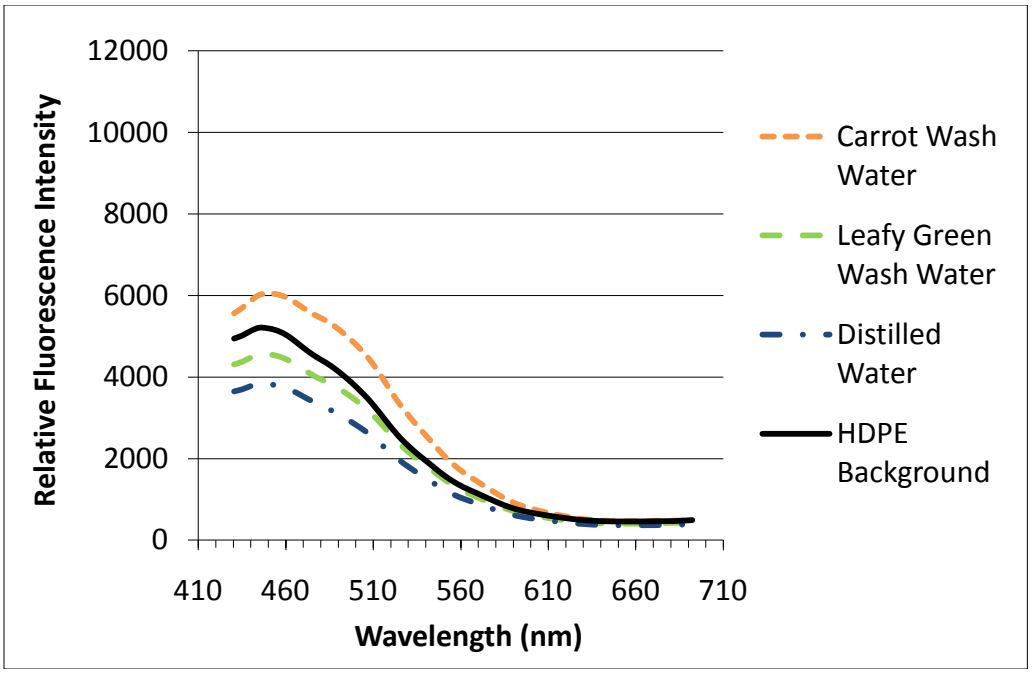

Figure 18: Representative fluorescence spectra of different fresh-cut produce processing wash water samples from Trial 1 on HDPE from 430.5 to 692.3 nm.

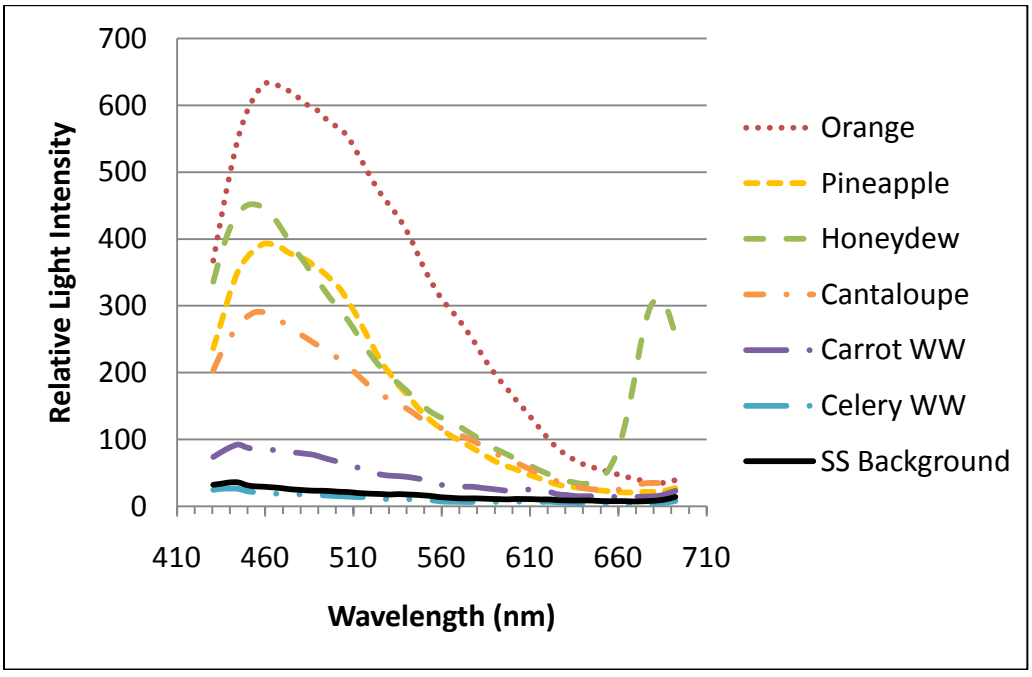

Figure 19: Representative fluorescence spectra of various fresh-cut produce processing exudates from Trial 2 on stainless steel from 430.5 to 692.3 nm.

All fresh-cut processing exudates tested were detectable from both backgrounds at certain wavebands with fluorescence imaging while none of the wash waters were detectable (Table 7). An RFI peak near 680 nm occurred for green pepper, honeydew, and cantaloupe exudates on HDPE and stainless steel indicating the presence of chlorophyll in these solutions. In Trial 1 the watermelon exudate's RFI amplitude was less than background from 430.5 to 520 nm and greater than background from 520 to 610 nm. A RFI peak unique from background occurred at 520 nm making the watermelon exudates detectable from 460-600 nm because the region with lower intensity than background was likely caused by lighting effects. The waveband range of detection for tested solutions was independent of background substrate material.

Table 7: Summary of possible wavelengths for detection of exudateas and wash waters collected from Company A with fluorescence imaging.

Test Substrate	Wavebands of Detectability
Cantaloupe, Green pepper, and Honeydew	430.5-600 nm, 660-692.3 nm
Carrot, Celery, and Leafy Green Wash Water	None
Orange and Pineapple	430.5-600 nm
Watermelon	460-600 nm

Discussion

There are many different wavelengths in the blue-green (460-600 nm) and red (670-700 nm) visible light range that could be utilized to detect fresh-cut cantaloupe exudates on stainless steel and HDPE with fluorescence imaging. Each cantaloupe tested had a variable level of ripeness, creating differences in exudate properties and RFI while not affecting wavelength range of detectability. Because of lighting variability in produce processing plants this flexibility enhances detection capabilities by letting a processor tailor the surface examination wavelengths for their own

facility. The device can examine surfaces at wavebands where background light intensity caused by ambient lights is lowest and optimize the sensitivity of fluorescence detection methods. The HDPE and SS coupons used were virgin material dissimilar to industrial processing surfaces to minimize background effects. While industrial processing surfaces can discolor and change after repeated use, this experiment focuses on the exudates themselves and where they may be detectable.

Cantaloupe exudate dilution droplets of 1-80 on stainless steel and 1-40 on HDPE were detectable with fluorescence imaging. After droplets dry, the detection limit was 1-80 on stainless steel and 1-160 on HDPE. Given that processing environments usually remain very wet after cleaning and sanitation, the results prior to drying are likely more relevant to imaging in produce processing plants.

The selected cleaners and sanitizers were not detectable with fluorescence imaging techniques. If a residual cleaner or sanitizer is left on a surface, either intentionally or unintentionally, it will not result in a false positive test, simplifying surface hygiene inspection. In particular, some sanitizers, such as chlorine or quaternary ammonia based solutions, are intentionally left on surfaces. The location of these cleaning and sanitizing solutions could be traced by adding food grade fluorescent dyes into their formulation. This capability would allow tracing cleaners and sanitizers to ensure agent removal or complete coverage of certain surfaces. Further studies are needed to determine the efficacy and feasibility of such practices.

The survey of samples collected from industry indicates fresh-cut produce processing exudates are detectable with fluorescence imaging, while produce wash waters are not. Fluorescence images in the blue-green range of the visible light

spectrum detected all fresh cut exudates, while images in the red range detected only cantaloupe, honeydew, and green pepper exudates. It is likely that exudates contain similar fluorescent compounds for the blue-green range and chlorophyll for the red range based on known fluorescent compounds. A wide range of detection wavebands exists for a fluorescence based hyperspectral imaging system to identify if these exudates are properly removed during cleaning and sanitation for the same reasons discussed in previous paragraphs. While initial results indicate difficulty in differentiating exudate type, the purpose of surface hygiene verification is to detect any possible contaminants left after cleaning and sanitation and then remove them.

Conclusion

These studies demonstrate the applicability of fluorescence based hyperspectral imaging techniques to detect fresh-cut processing related contaminants on stainless steel and high density polyethylene (HDPE). Results showed that the fluorescence emission spectrum peaks for fresh-cut cantaloupe exudates occurred at 459.1 and 682.8 nm with detection possible over large portions of the blue-green and red range of the visible light spectra. Similar results were found for fresh-cut processing exudates of pineapple, honeydew, pineapple, green pepper, and oranges. However, the selected cleaners, sanitizers, and wash waters examined in this study were not detectable with fluorescence imaging when placed on stainless steel or HDPE substrates. These laboratory findings will help identify specific wavebands to focus on during fluorescence based surface imaging in actual produce processing facilities with a portable imaging device. Choosing a set number of wavebands based on ambient lighting and potential contaminants fluorescence emission spectra will

enable an imaging device to assess surface hygiene rapidly over large surface areas. While this study focused on a select number of substances, future research can show if other potential contaminants or innocuous background substances are detectable from background surfaces at specific wavebands with fluorescence imaging.

Chapter 5: Portable Imaging Device Construction

Introduction

A portable, hyperspectral imaging device was developed to assess surface hygiene after cleaning and sanitation procedures. Given knowledge from previous studies and literature, this system was designed to detect contaminants such as fresh-cut processing exudates, plant material, biofilm build-up, fecal contamination, and potentially other unknown contaminants. Device components include an imaging system, fluorescence excitation source, battery supply, laptop with software, and touchscreen monitor for visualization. The device should allow operation by one person, function continuously for two hours, and scan surfaces at select wavebands in real-time. The project goal is to provide produce processors with a tool that can identify suspect surface sites and thereby improve surface hygiene immediately.

Materials and Methods

Device Construction

The image capturing system for the hyperspectral device is shown in Figure 20. A 12-bit charge coupled device (CCD) camera (Prosilica GC1380, Allied Vision Technologies Canada Inc., Burnaby, BC, Canada) is connected to specialized corrective optics (Channel Systems, Pinawa, MB, Canada) and a C-mount lens (S16mm, 2/3", Rainbow, Costa Mesa, CA) that focus incoming light. A 10-nm bandpass liquid crystal tunable filter (VariSpec, CRI, Inc., Woburn, MA) restricts the light detected by the CCD camera to a specific waveband between 400 and 720 nm.

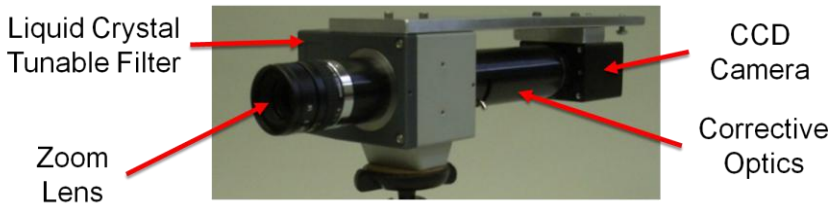

Figure 20: Image capturing system for the hyperspectral imaging device, including a CCD camera, lens, filter, and corrective optics.

The device's lighting assembly is shown in Figure 21. Violet light illumination for fluorescence excitation consists of four light emitting diodes (LED's) (LZ4-40UA10, LED Engin., Inc., Santa Clara, CA) with a peak intensity of 405 nm. The light-weight LED's provide sufficient energy for fluorescence excitation when compared to ultraviolet light sources and output light visible to humans that prevents accidental exposure that could damage human eyes. Finned, black aluminum LED holders (dealExtreme, Hung Hom, Kowloon, Hong Kong) dissipate generated heat. Diffraction lenses (dealExtreme) focus light onto the target surface to increase the excitation intensity. Current regulators (LuxDrive 3023-D-n-700, LEDdynamics, Randolph, VT) supply 700 mA to each LED. A manual switch turns the LED's on and off.

Figure 21: The lighting assembly used for the hyperspectral imaging device.

There are other support components important to the constructed device including a 20 nm bandpass filter controller (VariSpec, CRI, Inc., Woburn, MA), rechargeable batteries (Tenergy D Size 1000 mAh NiMH Button Top, Tenergy, Fremont, CA), a touchscreen monitor (Model 705TSV, Xenarc Technologies, Irvine, CA) for real-time visualization and user operation, a laptop (Thinkpad X61S, Lenovo, Morrisville, NC) for control of system components and image acquisition, and a backpack (Talon 44, Osprey Packs, Cortez, CO) that holds the batteries, filter controller, and laptop. An aluminum box with a hole for the camera lens protects and holds the optics and lighting assemblies and provides insulation. Reusable sorbent silica placed inside the aluminum box (P/N 1494SB99, SorbentSystems.com, Los Angeles, CA) keeps humidity low in wet processing environments. A tripod mount on the box's bottom (model 3130, Manfrotto, Bassano del Grappa, Vicenza, Italy) along with a tripod can be used to stabilize the box during image capture. The touchscreen attaches to the box's top (Figure 22) and a cable wrap protects the cords between the box to the backpack. The entire system allows the operator to move throughout a processing plant to image surfaces of interest (Figure 23).

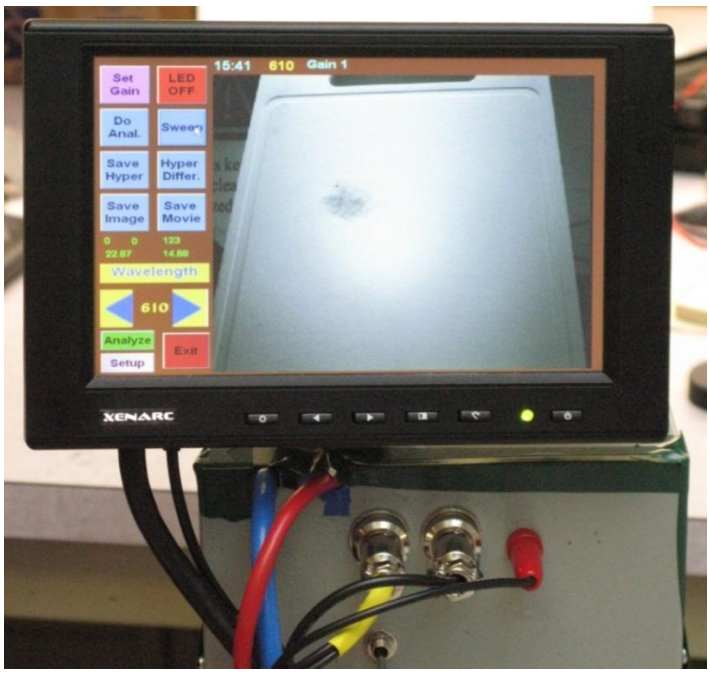

Figure 22: Hyperspectral imaging device touchscreen used for operation and visualization of results.

Figure 23: Prototype hyperspectral imaging devise in operation within a commercial produce processing facility to evaluate surface hygiene.

In-house software developed using Microsoft Visual Basic (version 6.0,

Microsoft. Seattle, WA) by USDA employees is used to control the imaging process.

Software functions include acquiring images, changing the filter's bandpass wavelength, adjusting gain and image acquisition rate, saving movies, monitoring filter temperature, loading pre-determined settings, and basic image analysis. The user can control these functions using buttons on a touchscreen interface that displays the time, image acquisition waveband, and gain (Figure 24). Many of these touchscreen buttons provide a unique functionality that helps an operator determine if a surface contains a contaminant (Table 8). Pixel resolution for the captured image, after binning 3 by 3 to reduce the signal to noise ratio, is 453 by 341 and each image can be saved as tiff files for later analysis. Images on the touchscreen display at 15 Hz to create a smooth video as the camera moves from side to side.

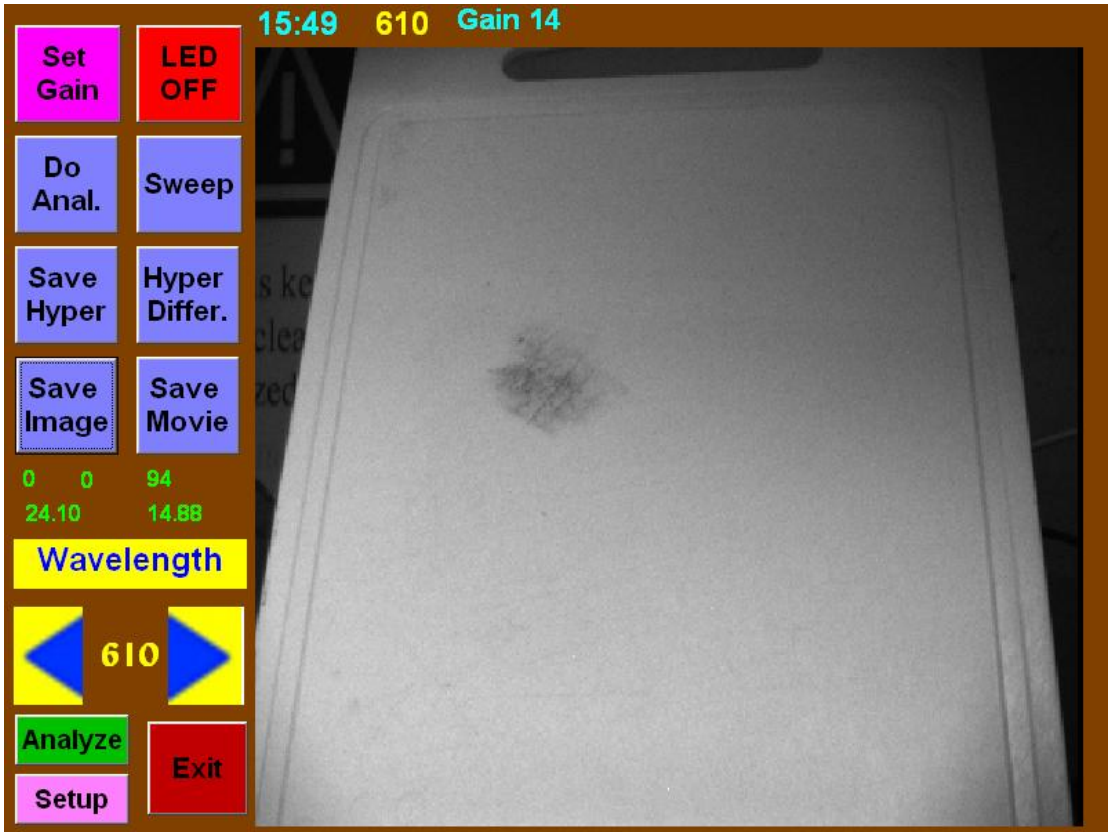

Figure 24: User interface screen developed for operation of the portable hyperspectral imaging device with touchscreen. Picture shown here is green leaf smear on white plastic cutting board imaged at 610 nm.

Table 8: Summary of buttons on user interface display.

Button	Function
Analyze	Takes user to separate analysis screen for image processing and review of previously acquired images
Do Anal.	Conduct rapid image analysis with pre-determined algorithm
Exit	Exit program and return to main screen
FPS	Change image acquisition rate as measured in frames per second
Hyper Differ.	Capture series of images from 460 to 720 nm at pre-determined waveband intervals with LED's on and off. Generates a series of difference BMP images where pixel intensities of the image without LED illumination are subtracted from those with LED illumination.
Save Image	Capture single image at one waveband
Save Movie	Capture series of images at one waveband at a selected time interval
Save Hyper	Capture series of images from 400 to 720 nm at pre-determined waveband intervals to generate a hyperspectral data set
Setup	Allows user to load file with desired system operational parameters
Set Gain	Adjust the gain at each waveband so average pixel intensity of image remains below 1096 on a 12 bit scale
Sweep	Display images at a selected number of pre-determined wavelengths at a selected update interval
Wavelength	Change center wavelength of tunable bandpass filter

The program also provides real-time updates on the temperature of the liquid crystal tunable filter. The filter characteristics degrade as temperature falls and the tunable filter may stop working if the temperature falls below 10 °C. Since most commercial produce processing facilities maintain a chilled processing environment

(0 to 4 °C) it's important the user to monitor the temperature to prevent damage during operation. Because the LED's generate heat that warms the camera system the filter temperature normally stays above 10 °C.

Functions available in the analysis screen include image subtraction, image ratios, and viewing previously saved images (Figure 25). Image subtraction and ratio analysis require the user select a primary and secondary wavelength of interest. The program then changes the primary wavelength for a set imaging technique or displays all imaging techniques for a set of primary and secondary wavelengths. This analysis allows the operator to review images and use processing techniques to optimize selection of wavebands and analysis techniques for routine inspections.

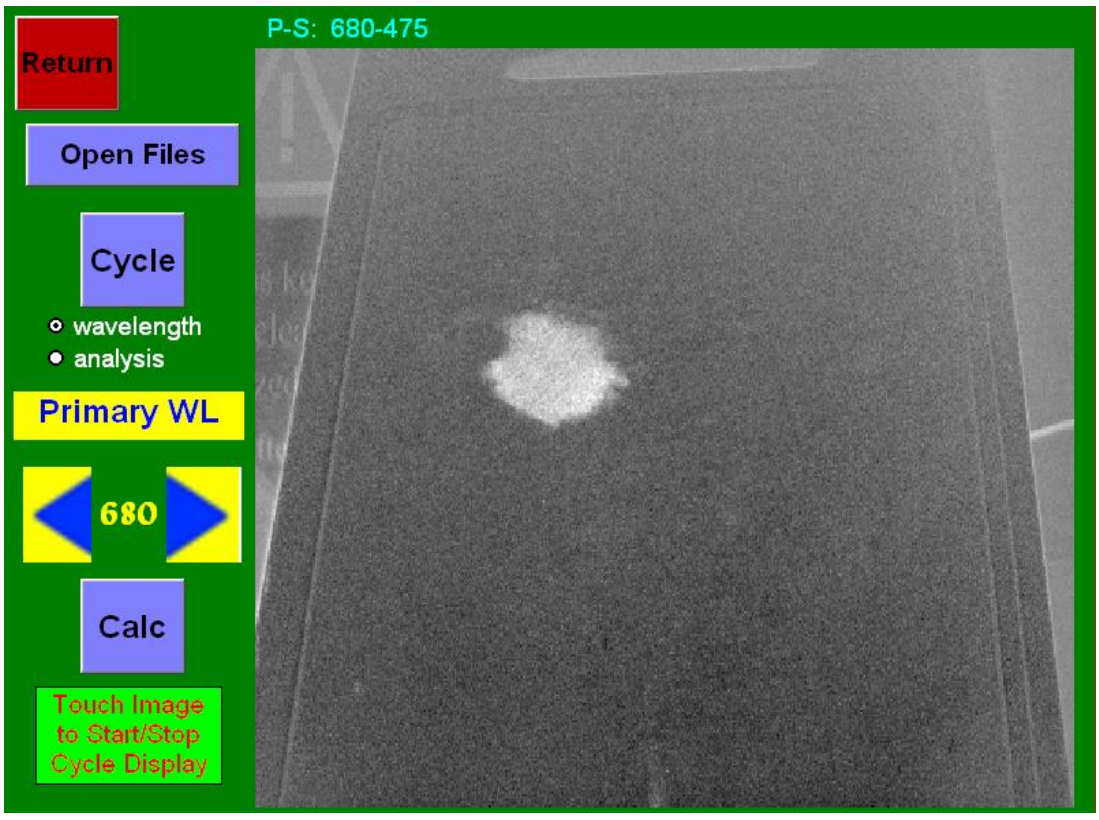

Figure 25: User interface screen developed for image processing techniques. Picture shown here is green leaf smear on a white plastic cutting board prepared in laboratory. A secondary image at 475 nm waveband is subtracted from a primary image at 680 nm waveband.

Lighting Assembly Testing

Basic spectral characterization of the violet LED's consisted of imaging a white surface in a dark room illuminated with the LED's. After hyperspectral series collection, the average intensity of a region of interest (ROI) on the white surface was calculated from 400 to 720 nm at 5 nm wavebands (Figure 26). The LED's emission peak occurred near 410 nm with noticeable intensity from 400 to 460 nm. At wavebands greater than 460 nm the LED's light intensity was negligible when compared to variations in ambient lighting.

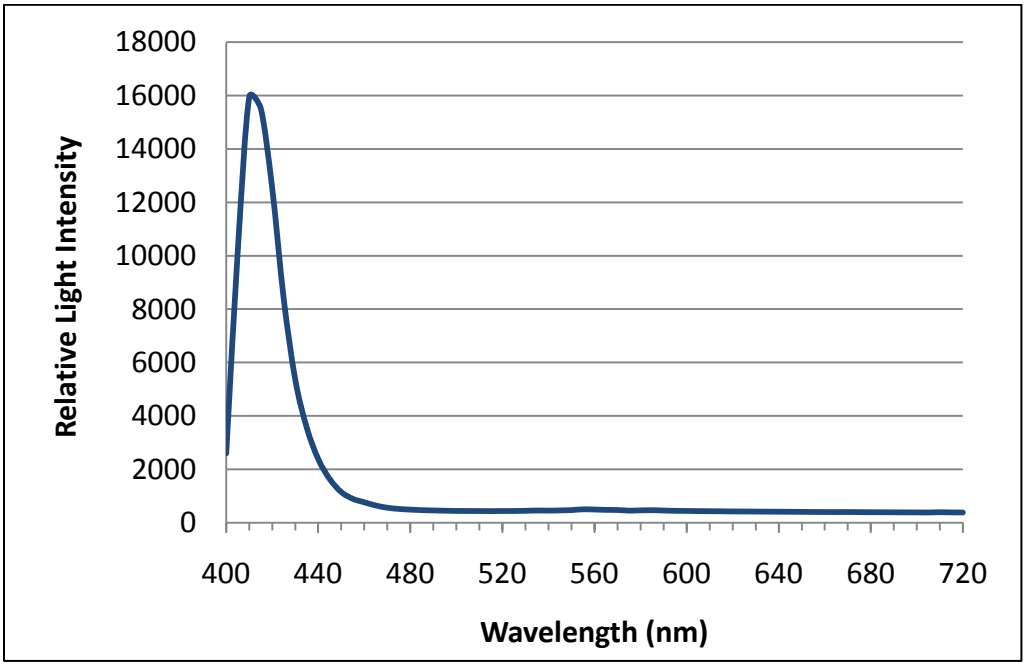

Figure 26: Relative light intensity of light emitting diodes on white background from 400 to 720 nm.

Selection of Wavebands for Surface Scanning

Turning off all lights in a processing plant to remove background signal would provide optimal conditions for fluorescence based imaging to detect potential contaminants. However, worker safety concerns prevent this from being feasible in

industry. By selecting specific wavebands for imaging the user can examine surfaces where background signal is minimized and optimize detection capabilities. Waveband selection also reduces the time required to survey surfaces allowing for greater coverage during use.

Factors that influenced waveband selection included the LED and ambient lighting emission spectra and the potential contaminants' fluorescence emission spectra. The measured relative maximum light intensity of the LED's emission spectrum ranged from 400-460 nm for LED illumination and the known emission spectrum relative maximums of fluorescent light bulbs range from 485-495nm, 535-555 nm, 575-635 nm, and 690-715 nm. An example that illustrates this point is the adjusted gain settings calculation when imaging a white HDPE cutting board in a commercial produce processing facility with ambient and LED illumination (Figure 27). To prevent signal saturation the system automatically adjusts the gain so that the average pixel intensity at each waveband is below 1096 on 12-bit scale. When light intensity on the examined surface, due to ambient or LED lighting, is greatest the gain is lowest and when light intensity is lowest the gain is highest. The ideal wavebands for fluorescent detection are those at which the gain is highest and background signal is lowest. Therefore, selected wavebands for surface examination should be between 460-475 nm, 515-530 nm, and 670-695 nm to achieve best detection sensitivity. As discussed in background sections and found in laboratory results, fresh-cut fruit and vegetable processing exudates fluoresce strongest between 460 and 580 nm, biofilms at 480 nm, chlorophyll-a at 680 nm, and fecal material at 675 nm. Given this

information a continuous three wavelength sweep of 475, 520, and 675 nm was chosen for scanning surfaces in Company A for fluorescent contaminants.

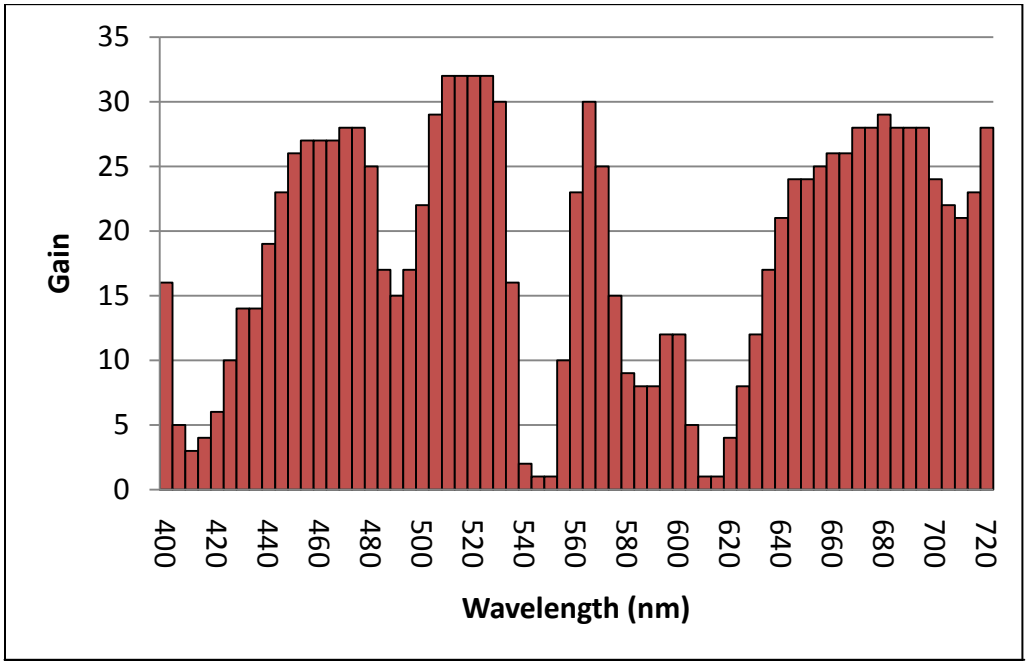

Figure 27: Example of automatically adjusted gain settings. Settings were generated by imaging HDPE cutting board in commercial processing plant. Gain was generated from 400 nm to 720 nm in 5 nm waveband increments with both violet LED and ambient light illumination.

Data Collection in Produce Processing Plant

The device was used to image surfaces at produce processing plant denoted as Company A after cleaning and sanitation and before production started. Initially the camera acquired images at 540 or 610 nm as these wavebands provided the best picture for the operator to identify what surface was being examined. Next the device imaged surfaces at 475, 520, and 675 nm in succession with LED illumination to locate potential fluorescent contaminants. Once a potentially fluorescent surface area was detected a hyperspectral series of images was acquired from 460 to 720 nm in 5 nm increments with the violet LED's on and off for comparison. After hyperspectral

series collection a series of difference images was displayed on the touchscreen that visually showed the user surfaces that contain actual fluorescent areas. By subtracting the pixel intensity of an image without LED illumination from one with LED illumination reflected light is negated and only fluorescent areas are shown. A digital camera (PowerShot G9, Canon, Lake Success, NY) captured color photographs of the examined surface area and a wide angle shot to document the camera's orientation and its distance from the object of interest. The time, surface location, surface type, surface function, samples taken, visual observations, and other notes for each location imaged were recorded for reference.

Surface Hygiene Testing in Produce Processing Plant

Select surface testing was conducted with a commercial ATP bioluminescence assay to evaluate surface hygiene. After the imaging system identified a site as potentially contaminated, an employee of Company A rubbed a swab (PocketSwab Plus, Charm Sciences Inc., Lawrence, MA) over an approximately 400 cm^2 surface area before placing it into a reagent solution. The light output of the reaction measured by a luminometer (novaLUM, Charm Sciences Inc.) in relative light units (RLU) indicated the amount of ATP present on the swab. If this test resulted in a non-zero reading then one or three subsequent tests of similar surfaces without any fluorescent areas were taken. Luminometer test results and captured images were then analyzed to determine if there was a correlation between fluorescent surfaces and higher ATPase assay results. All ATP bioluminescence test results were downloaded from the luminometer onto a computer for record keeping and analysis.

Chapter 6: Testing Device in Produce Processing Plant

Results and Discussion

The acquired images of different surfaces and equipment in a produce processing facility after cleaning and sanitation aided in surface hygiene evaluation. The hyperspectral system functioned properly for up to 2 hours and successfully detected some known and unknown contaminants as well as some anomalies not necessarily indicative of contamination. Suspect sites were identified in real-time and sometimes analyzed with ATP bioluminescence assays to further understand the nature of the contaminant. The following paragraphs summarize the key findings of these experiments.

Detection of Small Processing Debris

The portable system detected small pieces of vegetative matter not removed during cleaning and sanitation. Diced celery pieces not easily visible to the naked eye clearly appeared in an image acquired at a 680 nm waveband with LED illumination (Figure 28). The celery pieces settled into crevices where belt sections join and was not removed by cleaning and sanitation procedures. As a result of this finding, the company cleaned the belt again and removed the debris before beginning production.

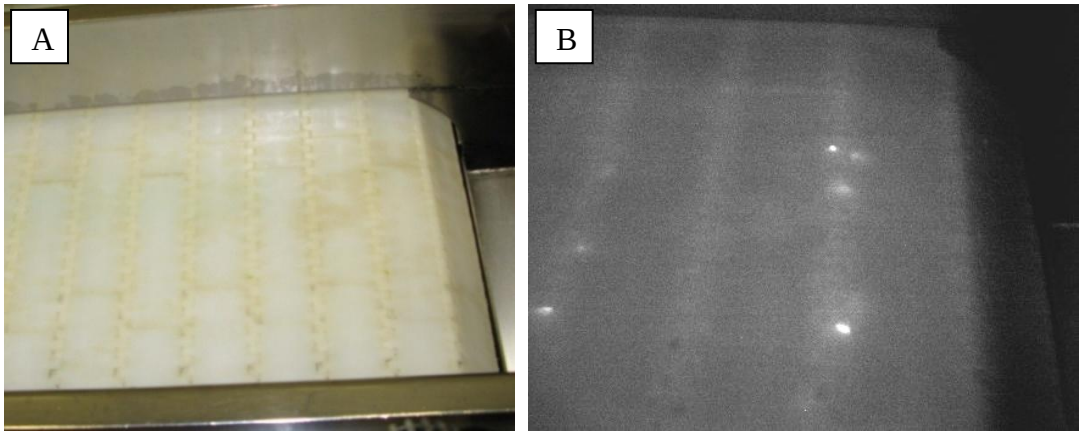

Figure 28: Images of celery sorting belt. Digital color photo (A) and image at 680 nm with violet LED illumination (B) acquired after cleaning and sanitation.

A similar pattern was noticed on a rotating vegetable slicer (Figure 29). Where the slicer blades meet the metal outer wheel, some plant debris accumulated and fluoresced strongly at 680 nm. Cleaning and sanitation failed to remove the vegetative matter from the slicing blade end and further cleaning was needed after imaging. The reflectance image acquired at 610 nm provided a more detailed picture of the slicer. By combining information from images at 610 and 680 nm the user can identify problem areas and take necessary measures to improve the surface hygiene.

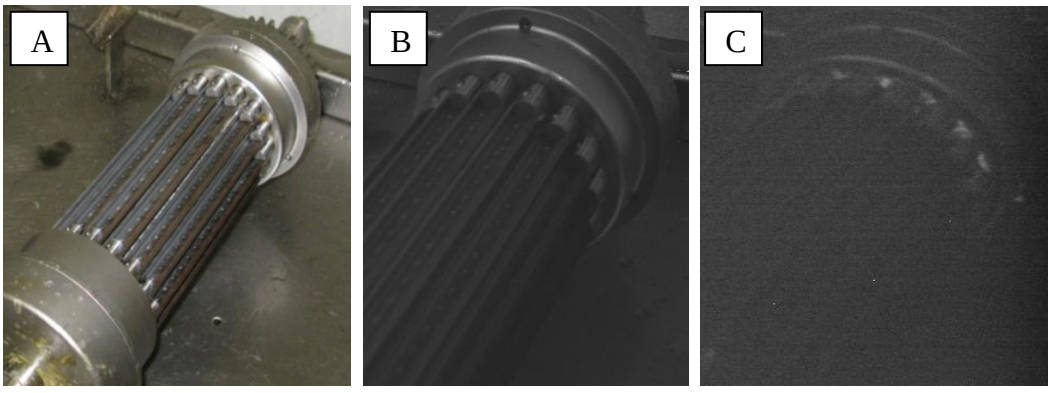

Figure 29: Images of rotating fresh-cut vegetable slicer. Digital color photo (A) and image with violet LED illumination at 610 nm (B) and 680 nm (C) acquired after cleaning and sanitation.

The device detected debris in a mechanical potato peeler not easily visible to the naked eye due to the brush's white color and poor lighting conditions (Figure 30). The camera revealed small, fluorescent potato debris on the brushes and rollers at the 520 nm waveband. While debris was also found at wavebands from 510-530, 550-570 and 660-690 nm, the 520 nm waveband provided the best sensitivity for detection. Similar results were seen when examining carrot peelers for debris.

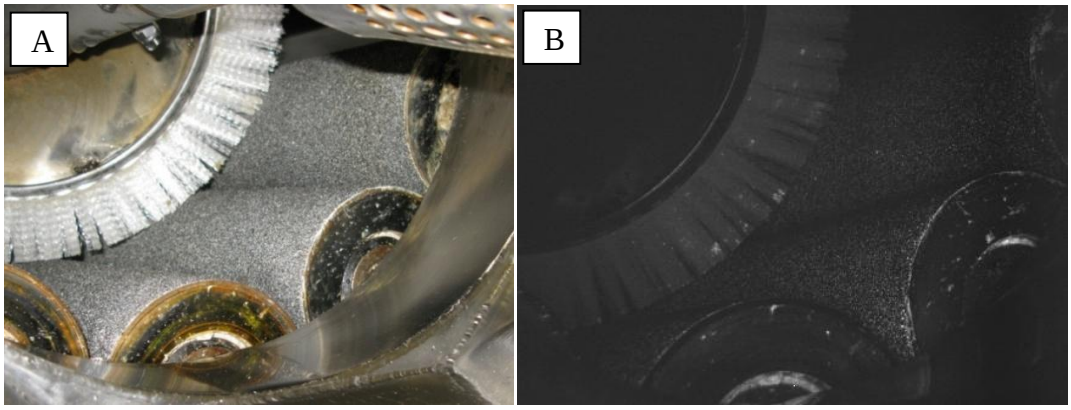

Figure 30: Images of industrial potato peeler. Digital color photo (A) and image with violet LED illumination at 520 nm (B) acquired after cleaning and sanitation.

Images of a mechanical belt that transports diced celery with LED illumination at a 675 nm waveband showed debris not removed by cleaning and sanitation (Figure 31). The debris, shown in the red box, was trapped between interlocking belt pieces and not easily visible to the naked eye.

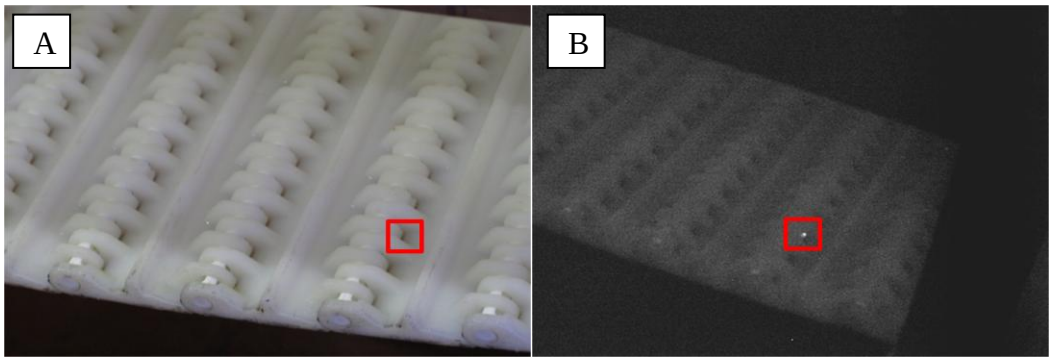

Figure 31: Images of celery transportation belt. Digital color photo (A) and image with violet LED illumination at 675 nm (B) acquired after cleaning and sanitation.

The portable hyperspectral device detected many types of processing debris left behind after cleaning and sanitation that were not be readily visible to the naked eye. Because different kinds of debris are more easily detected at different wavelengths a multispectral imaging at the three selected wavebands facilitates detection. Debris that remains after cleaning may serve as a reservoir for spoilage or pathogenic microbes to survive and transfer to products. By locating debris left behind, companies can immediately reclean problematic surfaces and make alterations to currently used cleaning and sanitation procedures to reduce the risk of microbial contamination.

Detection of Unknown Contaminants

The camera system also detected unknown potential contaminants not visible to the naked eye even upon close inspection. Such suspect sites could be tested with ATP bioluminescence assays before being recleaned. The ATP bioluminescence assays provide information about the nature and potential hazard of the contamination found. If a contaminant yields a high ATP count it may represent a biological hazard that could result future microbial contamination.

Difference images of a hanging plastic curtain that separates different produce processing areas in a commercial facility showed the locations of both known and unknown contaminants (Figure 32). At 530 nm some unknown brown compounds fluoresced, shown with the red square, and represent a potential concern because biofilms and fresh-cut processing exudates fluoresce at this waveband. At 680 nm debris from leafy green processing fluoresced strongly as seen with imaging system. After viewing these results, Company A permanently removed the curtain from the processing area.

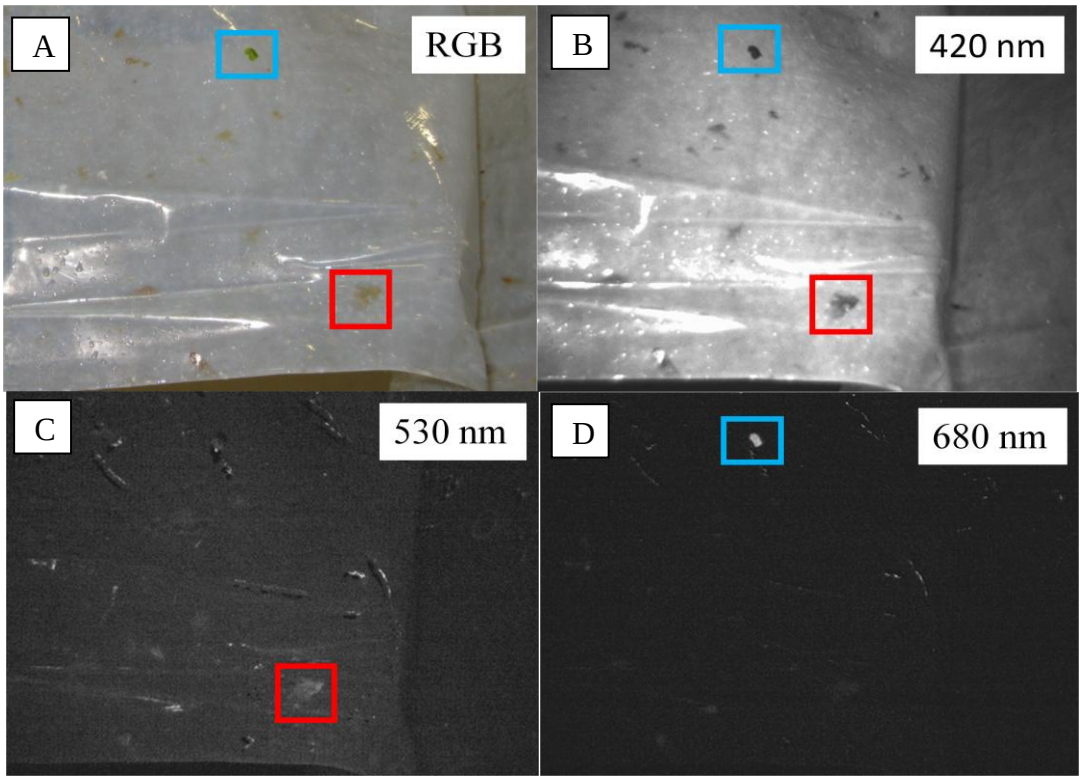

Figure 32: Images of hanging plastic curtain. Digital color photo (A) and difference images at 420 nm (B), 530 nm (C), and 680 nm (D) acquired after cleaning and sanitation.

Difference images of a packaged fresh-cut produce transport belt at 520 and 680 nm revealed that a noticeable brown accumulation in crevices of the white plastic fluoresced under violet light excitation (Figure 33). After viewing these images

Company A repeated cleaning and modified cleaning methods to prevent future accumulation on this type of belt.

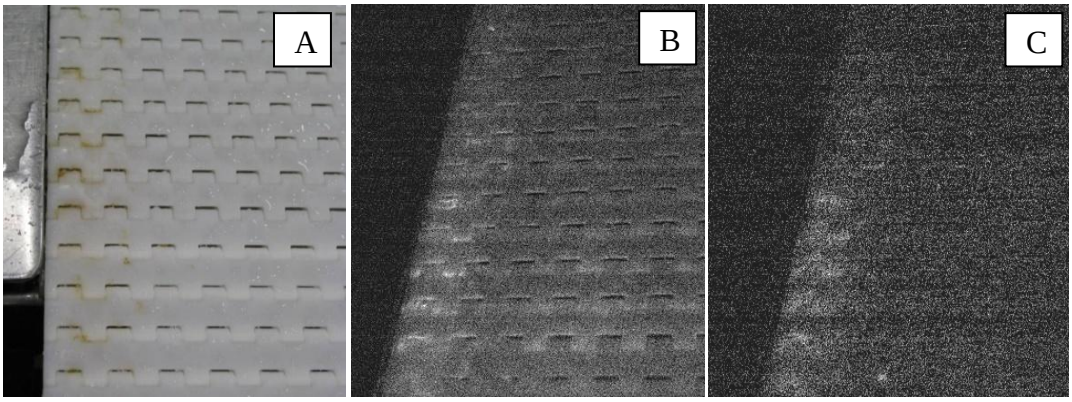

Figure 33: Images of plastic transportation belt. Digital color photo (A) and difference image at 520 nm (B) and 680 nm (C) acquired after cleaning and sanitation.

Fluorescence images of a cutting board used for fresh-cut preparation of leafy greens revealed a potential contaminant (Figure 34). With the naked eye and at the 610 nm waveband no contamination was detected on the HDPE cutting board under LED illumination while at 675 nm a small local contamination became visible to the user. After detecting the possible contamination, a surface sample was collected from the contaminated area and nearby areas with no fluorescent contaminants for ATP bioluminescence tests (Table 9). All areas sampled tested positive for ATP and did not differ from each other proving no correlation between this fluorescent location and ATP bioluminescence test results. However, the contaminated area might represent a general cleaning and sanitation procedure problem that was confirmed by the ATP bioluminescence test results. Given the results, Company A employees cleaned the problematic area again and made long term adjustments to their cleaning and sanitation procedures.

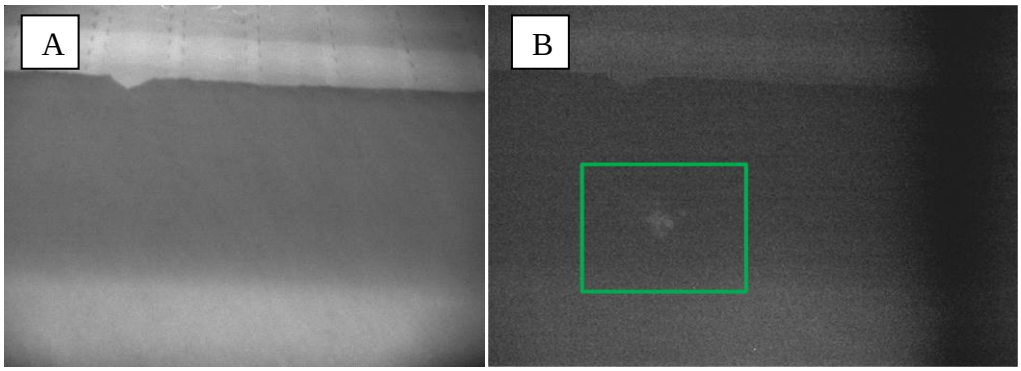

Figure 34: Images of lettuce cutting board. Images acquired at 610 nm (A) and 675 nm (B) with violet LED illumination after cleaning and sanitation.

Table 9: Results of ATP bioluminescence tests on a lettuce cutting board

Location	ATP test (RLU)
Lettuce cutting board over fluorescent area	2119
Lettuce cutting board random test area	2882
Lettuce cutting board random test area	3175
Lettuce cutting board random test area	2622

An apple slicer fluoresced noticeably on its inside surface both to the naked eye and at the 675 nm waveband under LED illumination (Figure 35). The locations of visible fluorescence are outlined in black in part B of Figure 35. ATP bioluminescence tests measured 9133 RLU for the slicer's fluorescent, inside wall (outlined in Figure 35) and 1336 RLU for the slicer's non-fluorescent, outside wall. Because the slicer directly contacts fresh-cut apple slices this represents a potential hazard that required immediate attention. The camera system revealed a fluorescent contaminant with a significant amount of ATP that would be missed without violet light illumination.

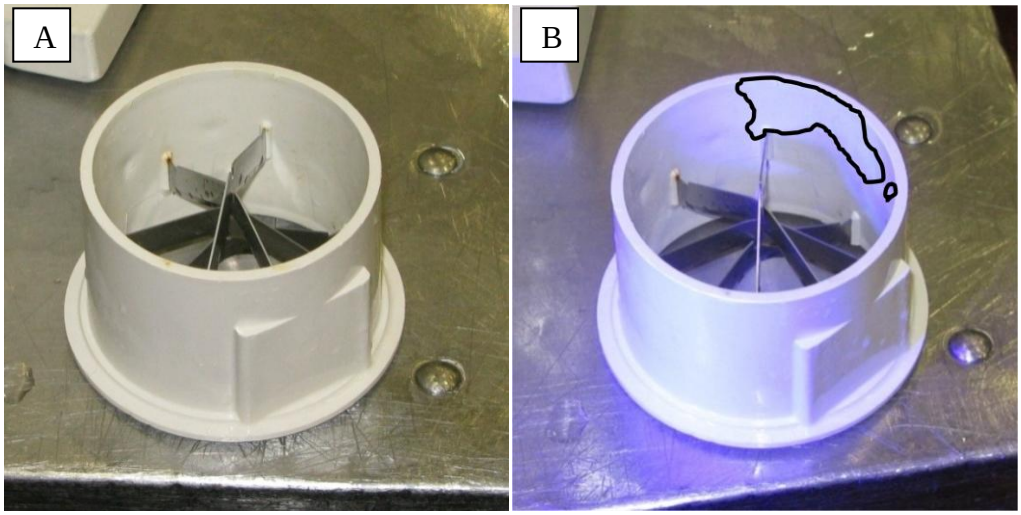

Figure 35: Images of an apple slicer. Digital color photos acquired with violet LED illumination off (A) and on (B) after cleaning and sanitation.

The camera system also identified a potential problem with a damaged HDPE cutting board that has higher fluorescence intensity than nearby areas (Figure 36). Small areas of fluorescence appeared at the 475 and 520 nm wavebands near the edge of the cutting board where the cutting board was visibly damaged. There was no noticeable fluorescence at 675 nm. ATP bioluminescence tests were taken of the fluorescent area and a non-fluorescent area nearby (Table 10). The damaged areas contain a higher ATP load than non-damaged areas nearby that do not fluoresce at 475 and 520 nm.

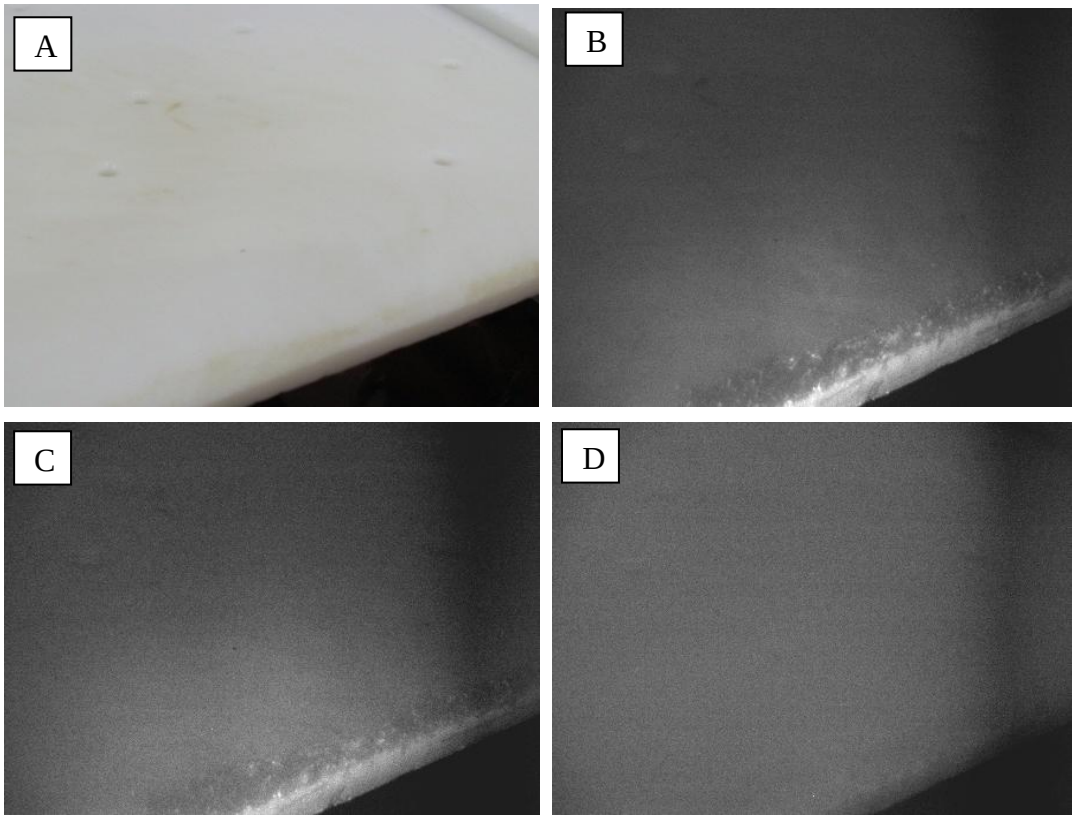

Figure 36: Images of white HDPE cutting board for fresh-cut vegetable products. Digital color photo (A) and image with violet LED illumination at 475 nm (B), 520 nm (C), and 675 nm (D) acquired after cleaning and sanitation.

Table 10: Results of ATP bioluminescence tests on a vegetable cutting board

Location	ATP test (RLU)
Cutting Board over damaged fluorescent area	298,260
Cutting Board over damaged fluorescent area	280,588
Nearby non-fluorescent area on cutting board	6532

To test whether the detected fluorescence resulted from the plastic's rough surface or a surface contaminant an HDPE coupon was damaged in the laboratory (Figure 37). On the coupon's edge an area (green box) fluoresced with slightly greater intensity after being damaged. The holes drilled into the HDPE also fluoresced due to their shape. In both test cases the fluorescence intensity magnitude was much less than the damaged cutting board observed at Company A. While damaged white

HDPE can appear fluorescent to the imaging system, the intensity observed in the commercial plant was likely due to some unknown contaminant.

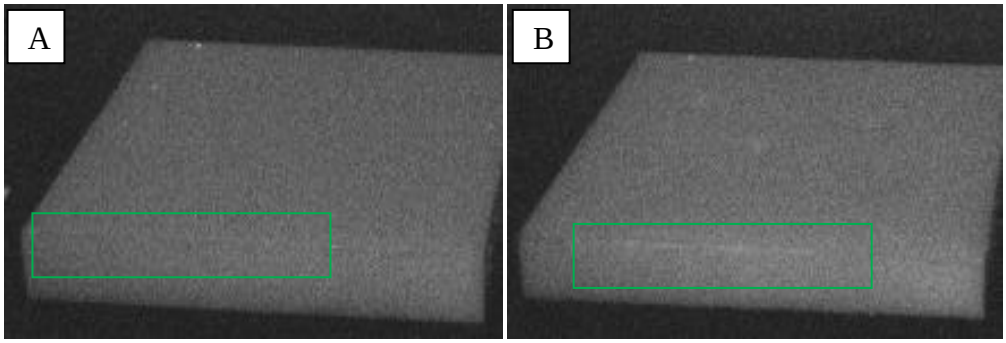

Figure 37: Images of HDPE coupon damaged in laboratory. Images acquired at 475 nm with violet LED illumination before (A) and after (B) drilling holes into coupon and sanding the edge with a belt sander.

These rough surfaces represent hard to clean areas that may serve as a reservoir for microorganisms. After viewing this data, Company A modified its standard procedures by increasing the amount of physical scrubbing on surfaces. On later visits the same fluorescence was seen at 475 and 520 nm wavebands on damaged tables, but ATP bioluminescence tests of these areas measured 3,050 RLU, a ten-fold decrease. The company made a dramatic improvement in cutting board surface hygiene by adding more mechanical action with an abrasive brush to aid removal of any potential contaminants on this problem area.

Detection of Potential Anomalies

Some areas found with the camera system were not necessarily indicative of poor surface hygiene, but appeared to fluoresce because of other factors. ATP tests of these locations were often negative (0 RLU) indicating these surfaces likely pose a low risk of causing microbial contamination. Through characterization of these anomalies, visual observation, and monitoring over time a company can prevent

taking unnecessary ATP tests and recleaning surfaces that are probably hygienic. These steps will improve the efficacy of the imaging device and save a company time and money by focusing on areas that have the greatest potential to cause problems.

Many anomalies derive from materials in the non-homogenous white HDPE cutting boards that display blue-green fluorescence. In one example (Figure 38) several locations fluoresce at 520 nm with greater intensity than surrounding areas. An ATP bioluminescence test of the highlighted blue area in Figure 38 measured 0 RLU while tests of two non-fluorescent areas nearby measured 1417 and 858 RLU respectively. Even after cleaning the same locations fluorescence at the 520 nm waveband. Similar results were found on other HDPE cutting boards with the fluorescent anomaly often visible to the naked eye.

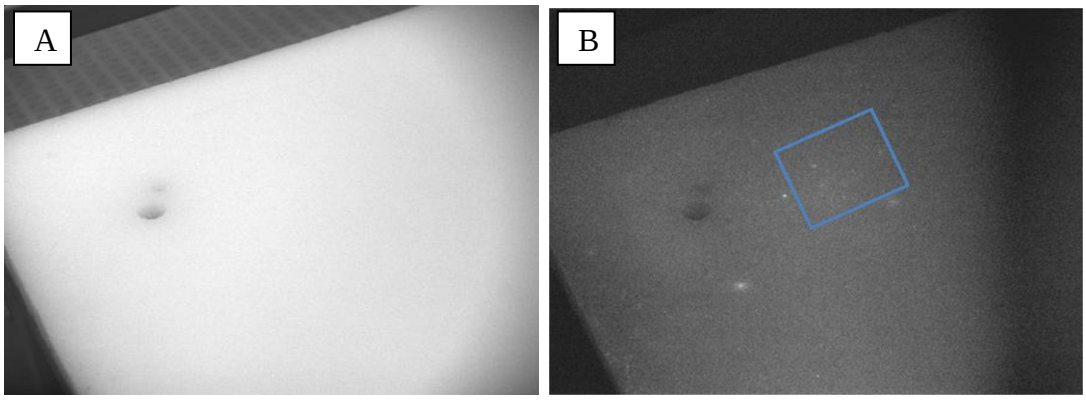

Figure 38: Images of lettuce cutting board. Images acquired at 610 nm (A) and 520 nm (B) with violet LED illumination after cleaning and sanitation.

Two plastic belt sections joined by different types of material fluoresced with greater intensity than surrounding areas even though an ATP bioluminescence test of the area measured 0 RLU (Figure 39). As a result of the material, waveband chosen, and LED illumination angle the surface fluoresced at wavebands where a potential contaminant would even though the surface was hygienic.

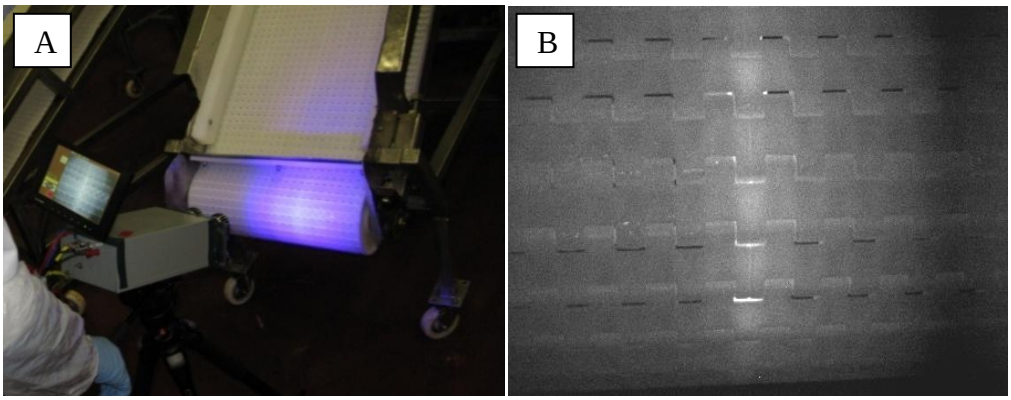

Figure 39: Images of fresh-cut celery transport belt. Digital color photo (A) and image with violet LED illumination at 520 nm (B) acquired after cleaning and sanitation.

Pooled water can produce another type of anomaly if the water refracts light, which gives the appearance of fluorescence (Figure 40). The bright locations at 520 nm resulted from sanitizing solution droplets reflecting light off their edge. An ATP bioluminescence test of the area measured 0 RLU while a random non-fluorescent area nearby measured 1394 RLU. These pooled solutions are common after sanitation and need to be considered when imaging.

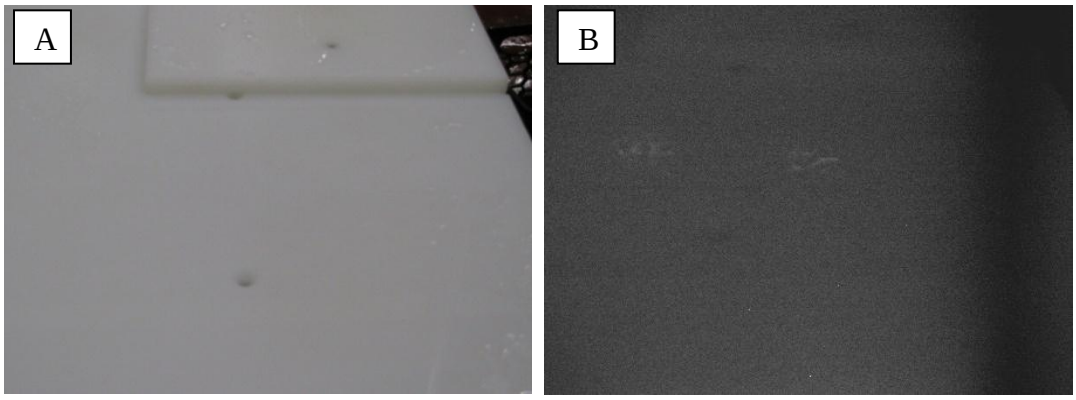

Figure 40: Images of plastic cutting board for fresh-cut fruit. Digital color photo (A) and difference image at 520 nm (B) acquired after cleaning and sanitation.

Methods to prevent these anomalies from being identified as high risk contaminants include moving the camera or employing visual inspection with the

naked eye. If an area that appears fluorescent moves when a surface is imaged from multiple perspectives it is likely caused by reflected or refracted light because fluorescence occurs independent of excitation source angle. Visual inspection can also provide information to the operator about a potential contaminant. While it is impossible to eliminate these anomalies, knowledge of their cause can prevent unnecessary testing and cleaning.

Conclusion

The portable hyperspectral imaging system successfully detected processing debris not readily visible with the naked eye with fluorescence imaging at 475, 520, and 675 nm wavebands. The system also found unknown contaminants that merited further inspection with ATP bioluminescent tests or culturing techniques. While some anomalies can represent false positives, the origin of most can be understood and further tests will help eliminate these false positives. With the data collected, Company A repeated cleaning and sanitizing steps on any problematic surfaces and adjusted standard procedures to improve future surface hygiene. Each visit drew more interest from quality assurance managers at Company A as they learned more about how the device worked, suggesting good potential for industry professionals to incorporate such a device into their surface sanitation verification procedures. The system successfully operated for two hours, but has limited mobility with its current construction. Future research is needed to determine the device's full capabilities and improve its mobility.

Chapter 7: Conclusion

A portable hyperspectral imaging device was developed to help improve hygiene verification after cleaning and sanitation procedures in commercial produce processing facilities. Lab tests demonstrated that it is possible to detect fresh-cut exudates on stainless steel and HDPE using fluorescence imaging. Optimal wavelengths for detection were determined to be 475, 520, and 675 nm when considering fluorescence response profiles and ambient lighting conditions. The device helped identify suspect sites that could then be tested with either ATP bioluminescence assays or culturing techniques to determine the possible hazard of the potential contaminant found. The portable hyperspectral imaging device improved the cleaning and sanitation practice in the produce company that participated in the research, and could become commercially viable with a lightweight, cost-effective version customized for the produce industry.

The existence of a USDA-ARS developed, commercial handheld, multispectral fluorescence based imaging prototype for use in the poultry processing industry suggests that a comparable device can be made for the produce industry. On the produce processing floor, it is anticipated that the quality assurance staff of a company, after basic training, will periodically examine contact surfaces for potential contaminants to reduce the risk of product contamination with pathogenic or spoilage microorganisms. Additionally, the device could be employed by regulatory agencies and/or third party auditors to monitor or conduct inspections for surface hygiene monitoring in the food and medical industries.

Appendices

Hyperspectral Measurements and Solution Properties

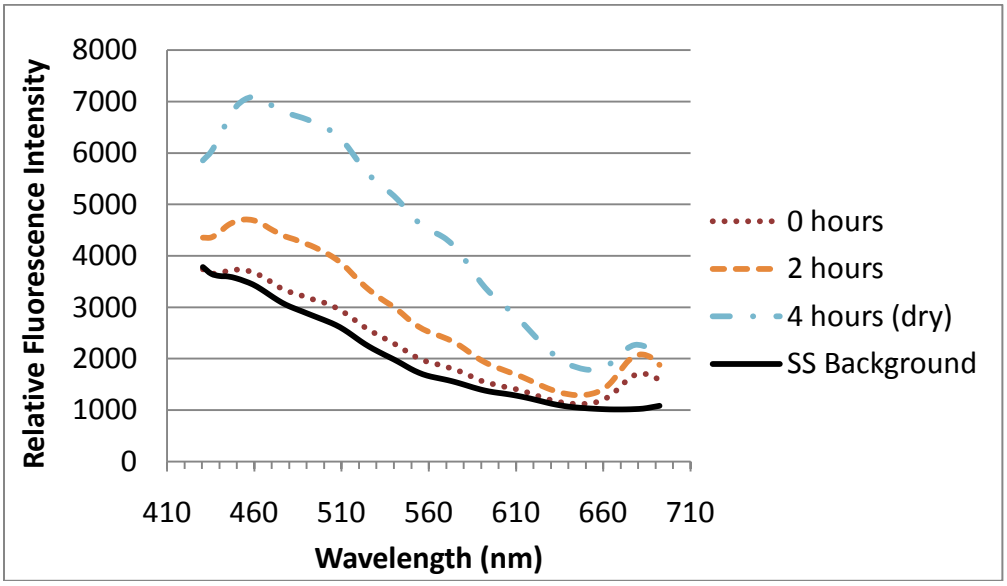

Figure A1: Representative fluorescence spectra of 1-10 fresh-cut cantaloupe exudate dilutions on stainless steel after drying for 0, 2, and 4 hours.

As the selected cantaloupe exudate dilution dries, the amplitude of its emission spectra increases. While the solution was generally detectable from 460 to 630nm and 670 to 700 nm, it only became detectable from 430.5 to 460 nm after 2 hours of drying time.

Table A1: Solutions property ranges of fresh-cut produce exudates tested.

Produce Type	Total Solids (%)	Soluble Solids (°Brix)
Cantaloupe in Lab	6.229-13.619	6.75-12.5
Honeydew in Lab	10.433-10.577	6.71-10.42
Industry Cantaloupe	3.6688-10.025	3.5-13.75
Industry Honeydew	7.264-8.128	4.13-8.75
Industry Salsa Juice	4.534	4-4.5
Industry Pineapple	6.797-11.778	7.5-10.75
Industry Green Pepper	0.598-0.776	0.25-0.5
Industry Watermelon	9.433	9.5
Industry Orange	12.5426	13.5

Bibliography

Ariana D, Guyer DE & Shrestha B. 2006. Integrating multispectral reflectance and fluorescence imaging for defect detection on apples. Computers and Electronics in Agriculture 50:148-161.

Aycicek H, Oguz U & Karci K. 2006. Comparison of results of ATP bioluminescence and traditional hygiene swabbing methods for the determination of surface cleanliness at a hospital kitchen. International Journal of Hygiene and Environmental Health 209:203-206.

Banada PP, Huff K, Bae E, Rajwa B, Aroonnual A, Bayraktar B, Adil A, Robinson JP, Hirleman ED & Bhunia AK. 2009. Label-free detection of multiple bacterial pathogens using light-scattering sensor. Biosensors & Bioelectronics 24:1685-1692.

Behravesh CB, Mody RK, Jungk J, Gaul L, Redd JT, Chen S, Cosgrove S, Hedican E, Sweat D, Chávez-Hauser L, Snow SL, Hanson H, Nguyen T-A, Sodha SV, Boore AL, Russo E, Mikoleit M, Theobald L, Gerner-Smidt P, Hoekstra RM, Angulo FJ, Swerdlow DL, Tauxe RV, Griffin PM & Williams IT. 2011. 2008 Outbreak of *Salmonella* saintpaul infections associated with raw produce. New England Journal of Medicine 364:918-27.

Bidol SA, Daly ER, Rickert RE, Hill TA, Al Khaldi S, Taylor TH, Jr., Lynch MF, Painter JA, Braden CR, Yu PA, Demma L, Behravesh CB, Olson CK, Greene SK, Schmitz AM, Blaney DD & Gershman M. 2007. Multistate outbreaks of *Salmonella* infections associated with raw tomatoes eaten in restaurants - United States, 2005-2006. Morbidity and Mortality Weekly Report 56:909-911.

Borchert D. 2004. Cleaning Validation. GMP Manual (UP04). Maas & Peither - GMP Publishing.

Brody SS. 1958. New excited state of chlorophyll. Science 128:839-839.

Buck JW, Walcott RR & Beuchat LR. 2003. Recent trends in microbiological safety of fruits and vegetables. Online. Plant Health Progress. Available from APSnet (APSnet.org). Posted Dec 20, 2002.

Centers for Disease Control and Prevention. 2002. Multistate outbreaks of Salmonella serotype Poona infections associated with eating cantaloupe from Mexico: United States and Canada, 2000-2002. Morbidity and Mortality Weekly Report 51(46):1044-1047.

Centers for Disease Control and Prevention. 2008. Outbreak of *Salmonella* Serotype Saintpaul Infections Associated with Multiple Raw Produce Items --- United States, 2008. Morbidity and Mortality Weekly Report 57(34):929-934.

Centers for Disease Control and Prevention. 2010a. Investigation Update: Multistate Outbreak of Human *E. coli* O145 Infections Linked to Shredded Romaine Lettuce from a Single Processing Facility. [Internet]. [Updated 2010 May 21; Accessed 2011 Jan 8]. Available from: http://www.cdc.gov/ecoli/2010/ecoli_o145/index.html.

Centers for Disease Control and Prevention. 2010b. Investigation Update: Multistate Outbreak of Human *Salmonella* Newport Infections Linked to Raw Alfalfa

Sprouts. [Internet]. [Updated 2010 June 29; Accessed 2011 Jan 8]. Available from: http://www.cdc.gov/salmonella/newport/index.html.
Centers for Disease Control and Prevention. 2011. Investigation Update: Multistate Outbreak of Human *Salmonella* I 4,[5],12:i:- Infections Linked to Alfalfa Sprouts. [Internet]. [Updated February 10, 2011; Accessed 2011 March 6]. Available from: http://www.cdc.gov/salmonella/i4512i-/011411/index.html.
Chappelle EW, McMurtrey JE & Kim MS. 1991. Identification of the pigment responsible for the blue fluorescence band in the laser induced fluorescence (LIF) spectra of green plants, and the potential use of this band in remotely estimating rates of photosynthesis. Remote Sensing of Environment 36:213-218.
Cho B, Kim MS, Chao K, Lawrence K, Park B & Kim K. 2009. Detection of Fecal Residue on Poultry Carcasses by Laser-Induced Fluorescence Imaging. Journal of Food Science 74:E154-E159.
Cho BK, Chen YR & Kim MS. 2007. Multispectral detection of organic residues on poultry processing plant equipment based on hyperspectral reflectance imaging technique. Computers and Electronics in Agriculture 57:177-189.
Cook R. 2007. Trends in the Marketing of Fresh Produce and Fresh-cut Products. Agricultural Issues Center, University of California.
Costa PD, Andrade NJd, Passos FJV, Brandão SCC & Rodrigues CGF. 2004. ATP - bioluminescence as a technique to evaluate the microbiological quality of water in food industry. Brazilian Archives of Biology and Technology 47:399-405.
Donlan RM & Costerton JW. 2002. Biofilms: Survival mechanisms of clinically relevant microorganisms. Clinical Microbiology Reviews 15:167-193.
Fan XT, Annous BA, Keskinen LA & Mattheis JP. 2009. Use of chemical sanitizers to reduce microbial populations and maintain quality of whole and fresh-cut cantaloupe. Journal of Food Protection 72:2453-2460.
Fatemi P & Frank JF. 1999. Inactivation of *Listeria monocytogenes*/*Pseudomonas* Biofilms by Peracid Sanitizers. Journal of Food Protection 62:761-765.
Fry SC. 1979. Phenolic components of the primary cell-wall and their possible role in hormonal-regulation of growth. Planta 146:343-351.
Fry SC. 1982. Phenolic components of the primary cell wall. Biochemical Journal 203:493-504.
Gerner-Smidt P & Whichard JM. 2007. Foodborne disease trends and reports. Foodborne Pathogens and Disease 4:391-394.
Gracias KS & McKillip JL. 2004. A review of conventional detection and enumeration methods for pathogenic bacteria in food. Canadian Journal of Microbiology 50:883-890.
Guilbault GC. 1990a. Assay of Organic Compounds. In: Guilbault, G. C., editor. Practical Fluorescence. 2nd ed. New York: Marcel Dekker, Inc. p. 231-366.
Guilbault GG. 1990b. General Aspects of Luminescence Spectroscopy. In: Guilbault, G. C., editor. Practical Fluorescence. 2nd ed. New York: Marcel Dekker, Inc. p. 1-40.

Hahn F, Lopez I & Hernandez G. 2004. Spectral detection and neural network discrimination of *Rhizopus stolonifer* spores on red tomatoes. Biosystems Engineering 89:93-99.

Hennessy TW, Hedberg CW, Slutsker L, White KE, BesserWiek JM, Moen ME, Feldman J, Coleman WW, Edmonson LM, MacDonald KL, Osterholm MT, Belongia E, Boxrud D, Boyer W, Danila R, Korlath J, Leano F, Mills W, Soler J, Sullivan M, Deling M, Geisen P, Kontz C, Elfering K, Krueger W, Masso T, Mitchell MF, Vought K, Duran A, Harrell F, Jirele K, Krivitsky A, Manresa H, Mars R, Nierman M, Schwab A, Sedzielarz F, Tillman F, Wagner D, Wieneke D & Price C. 1996. A national outbreak of Salmonella enteritidis infections from ice cream. New England Journal of Medicine 334:1281-1286.

Hoffmann S, Ficshbeck P, Krupnici A & McWilliams M. 2007. Using expert ellicitation to link foodborne illnesses in the United States to foods. Journal of Food Protection 70:1220-1229.

Institute of Food Technologists & Food and Drug Administration. 2001. Analysis and evaluation of preventive control measures for the control and reduction/ elimination of microbial hazards on fresh and fresh-cut produce.

Jiang L, Zhu, B., Jing, H., Chen, X., Rao, X., and Tao, Y. 2007. Gaussian mixture model based walnut shell and meat classification in hyperspectral fluorescence imagery. Transactions of the ASABE 50:153-160.

Jun W, Kim M, Lee K, Millner P & Chao K. 2009. Assessment of bacterial biofilm on stainless steel by hyperspectral fluorescence imaging. Sensing and Instrumentation for Food Quality and Safety 3:41-48.

Jun W, Kim MS, Cho B-K, Millner PD, Chao K & Chan DE. 2010. Microbial biofilm detection on food contact surfaces by macro-scale fluorescence imaging. Journal of Food Engineering 99:314-322.

Kim MS, Chen YR & Mehl P. 2001. Hyperspectral reflectance and fluorescence imaging system for food quality and safety. Transactions of the ASAE 44: 721-729.

Kim MS, Cho BK, Chao KL, Lefcourt AM, Liu YL & Chen YR. 2006. Detection of contaminants on poultry processing plant equipment using laser-induced fluorescence imaging. In: Lee, S. S., Lee, J. H., Park, I. K., Song, S. J. & Choi, M. Y., editors. Advanced Nondestructive Evaluation I, Pts 1 and 2, Proceedings. Zurich-Uetikon: Trans Tech Publications Ltd. p. 1157-1162.

Kim MS, Lefcourt AM, Chao K, Chen YR, Kim I & Chan DE. 2002. Multispectral detection of fecal contamination on apples based on hyperspectral imagery. Part I. Application of visible and near-infrared reflectance imaging. Transactions of the ASAE 45:2027-2037.

Kim MS, Lefcourt AM & Chen YR. 2003. Optimal fluorescence excitation and emission bands for detection of fecal contamination. Journal of Food Protection 66:1198-1207.

Kim MS, Lefcourt AM, Chen YR & Tao Y. 2005. Automated detection of fecal contamination of apples based on multispectral fluorescence image fusion. Journal of Food Engineering 71:85-91.

Kim MS, Lefcourt, A.M., Chen, Y.R., Kim, I., Chao, K., and Chan, D.E. 2002. Multispectral detection of fecal contamination on apples based on hyperspectral imagery-part II: application of fluorescence imaging. Transactions of the ASAE 45:2039-2047.

Kok B. 1976. Photosynthesis: The path of energy. In: Plant Biocehmistry. New York: Academic. p. 846-883.

Kumar CG & Anand SK. 1998. Significance of microbial biofilms in food industry: a review. International Journal of Food Microbiology 42:9-27.

Kvenberg J, Stolfa P, Stringfellow D & Spencer Garrett E. 2000. HACCP development and regulatory assessment in the United States of America. Food Control 11:387-401.

Lakowicz JR. 2006. Principles of Fluorescence Spectroscopy,Third ed. New York: Springer Science + Business Media, LLC.

Landry L, Phan Q, Kelly S, Phillips K, Onofrey S, Daly ER, Talbot EA, Fage M, Deasy M, Spayne M, Lynch M & Olson CK. 2007. *Salmonella* Oranienburg infections associated with fruit salad served in health-care facilities - Northeastern United States and Canada, 2006. Morbidity and Mortality Weekly Report 56:1025-1028.

Lee K, Kang S, Delwiche S, Kim M & Noh S. 2008. Correlation analysis of hyperspectral imagery for multispectral wavelength selection for detection of defects on apples. Sensing and Instrumentation for Food Quality and Safety 2:90-96.

Lefcourt AM, Kim MS & Chen YR. 2003. Automated detection of fecal contamination of apples by multispectral laser-induced fluorescence imaging. Applied Optics 42:3935-3943.

Liu YL, Chen YR, Kim MS, Chan DE & Lefcourt AM. 2007. Development of simple algorithms for the detection of fecal contaminants on apples from visible/near infrared hyperspectral reflectance imaging. Journal of Food Engineering 81:412-418.

Llewellyn LJ, Evans MR & Palmer SR. 1998. Use of sequential case-control studies to investigate a community salmonella outbreak in Wales. Journal of Epidemiology and Community Health 52:272-276.

Llères D, Swift S & Lamond AI. 2007. Detecting Protein-Protein Interactions In Vivo with FRET using Multiphoton Fluorescence Lifetime Imaging Microscopy (FLIM). Current Protocols in Cytometry. 42:12.10.1–12.10.19.

Lo YM, Wang J, Lala G, Liu T & Wiederoder MS. 2010. Sensors: Bioluminescence. In: Heldman, DR. editor. Encyclopedia of Agricultural, Food, and Biological Engineering, 2nd ed. New York: Taylor & Francis 1:1, p. 1520-1524.

Lundquist K, Josefsson B & Nyquist G. 1978. Analysis of Lignin Products by Fluorescence Spectroscopy. Holzforschung 32:27-32.

Maukonen J, Mättö J, Wirtanen G, Raaska L, Mattila-Sandholm T & Saarela M. 2003. Methodologies for the characterization of microbes in industrial environments: a review. Journal of Industrial Microbiology and Biotechnology 30:327-356.

Mehl PM, Chao K, Kim M & Chen YR. 2002. Detection of defects on selected apple cultivars using hyperspectral and multispectral image analysis. Applied Engineering in Agriculture 18:219-226.

Mehl PM, Chen YR, Kim MS & Chan DE. 2004. Development of hyperspectral imaging technique for the detection of apple surface defects and contaminations. Journal of Food Engineering 61:67-81.

Mintel: Bagged Salad and Salad Dressings - US - July 2008 [Internet]. Chicago, IL: Mintel International Group Ltd.; July 2008. [Accessed 2011 Jan 15]. Available from: http://oxygen.mintel.com.

Mintel: Fruit - 2009 - US - February 2009 Market Size and Forcast [Internet]. Chicago, IL: Mintel International Group Ltd.; February 2009. [Accessed 2011 Jan 15]. Available from: http://oxygen.mintel.com.

Morgan D, Newman CP, Hutchinson DN, Walker AM, Rowe B & Majid F. 1993. Verotoxin-producing *Escherichia coli* O157:H7 infections associated with the consumption of yogurt. Epidemiology and Infection 111:181-187.

Niemira BA. 2007. Irradiation sensitivity of planktonic and biofilm-associated Escherichia coli O157 : H7 isolates is influenced by culture conditions. Applied and Environmental Microbiology 73:3239-3244.

Nivens DE, Co BM & Franklin MJ. 2009. Sampling and quantification of biofilms on food processing equipment. Biofilms in the food and beverage industries. CRC Press.

Park B, Lawrence, K.C., Windham, W.R., & Buhr, R.J. 2002. Hyperspectral imaging for detecting fecal and ingesta contamination on poultry carcasses. Transactions of the ASAE 45:2017-2026.

Perishables Group: Fresh Cut Produce in the U.S.A [Internet]. Chicago, Il: Perishables Group. Oct 8, 2010. [Accessed 2011 Jan 5]. Available from www.perishablesgroup.com.

Poulsen LV. 1999. Microbial Biofilm in Food Processing. Lebensmittel-Wissenschaft und-Technologie 32:321-326.

Promega Corporation: An Introduction to Fluorescence Measurements: Variables of Fluorescence [Internet]. Sunnyvale, CA: Promega Corporation; 2011 [Accessed 2011 March 12]. Available from http://www.mail.turnerbiosystems.com.

Pérez-Rodríguez F, Valero A, Carrasco E, García RM & Zurera G. 2008. Understanding and modelling bacterial transfer to foods: a review. Trends in Food Science & Technology 19:131-144.

Qin J, Burks T, Kim M, Chao K & Ritenour M. 2008. Citrus canker detection using hyperspectral reflectance imaging and PCA-based image classification method. Sensing and Instrumentation for Food Quality and Safety 2:168-177.

Reij MW, Den Aantrekker ED & Microbio IERA. 2004. Recontamination as a source of pathogens in processed foods. International Journal of Food Microbiology 91:1-11.

Riddle D. 2006. Coral Coloration: Fluorescence: Part 1. Advanced Aquarist Magazine Online [serial conline].5. Available from Advanced Aquarist (www.advanceaquarist.com). Posted Sep 15, 2006.

Scallan E, Griffin P, Angulo F, Tauxe R & Hoekstra R. 2011. Foodborne illness acquired in the United States - unspecified agents. Emergin Infectious Diseases 17: 16-22.

Scharff RL. 2010. Health-Related Costs from Foodborne Illness in the United States. Produce Safety Project. p. 1-29.

Silagyi K, Kim SH, Lo YM & Wei CI. 2009. Production of biofilm and quorum sensing by Escherichia coli O157:H7 and its transfer from contact surfaces to meat, poultry, ready-to-eat deli, and produce products. Food Microbiology 26:514-519.

U.S. Department of Agriculture & U.S. Department of Health and Human Services. 2010. Dietary Guidelines for Americans 2010. [Internet]. [Updated 2011 Jan 31; Accessed 2011 Feb 6]. Available from: http://www.cnpp.usda.gov/DGAs2010-PolicyDocument.htm.

U.S. Food and Drug Administration. 2006. Krisp-Pak Company, Inc. Recalls Fresh Cut Fruit Because of Possible Health Risk. [Internet]. [Updated 2010 Jan 4; Accessed 2011 Feb 6]. Available from: http://www.fda.gov/Safety/Recalls/ArchiveRecalls/2006/ucm112062.htm.

U.S. Food and Drug Administration. 2007. Dole Fresh Vegetables Announces Voluntary Recall of 'Dole Hearts Delight' Packaged Salads. [Internet]. [Accessed 2011 Feb 6]. Available from: http://www.fda.gov/oc/po/firmrecalls/dole09_07.html.

U.S. Food and Drug Administration. 2008a. FDA Warns of Salmonella Risk with Cantaloupes from Agropecuaria Montelibano. [Internet]. [Updated 2009 Aug 26; Accessed 2011 Feb 6]. Available from: http://www.fda.gov/Food/NewsEvents/ConstituentUpdates/ucm047425.htm.

U.S. Food and Drug Administration. 2008b. Guidance for Industry: Guide to Minimize Microbial Food Safety Hazards of Fresh-cut Fruits and Vegetables. [Internet]. [Updated 2009 July 10; Accessed 2010 May 13]. Available from: http://www.fda.gov/food/guidancecomplianceregulatoryinformation/guidancedocuments/produceandplanproducts/ucm064458.htm.

U.S. Food and Drug Administration. 2011a. Del Monte Fresh Produce Voluntarily Recalls Cantaloupes Because Of Possible Health Risk. [Internet]. [Updated 2011 March 3; Accessed 2011 March 6]. Available from: http://www.fda.gov/Safety/Recalls/ucm248103.htm.

U.S. Food and Drug Administration. 2011b. Guidance for Industry: Letter to Firms that Grow, Harvest, Sort, Pack, or Ship Fresh Cilantro. [Internet]. [Updated 2011 Apr 1; Accessed 2011 April 15]. Available from: http://www.fda.gov/Food/GuidanceComplianceRegulatoryInformation/GuidanceDocuments/ProduceandPlanProducts/ucm249401.htm.

U.S. Food and Drug Administration. 2011c. Sabor Farms Recalls Four Brands Of Cilantro Because Of Possible Health Risk. [Internet]. [Updated 2011 Jan 31; Accessed 2011 Feb 6]. Available from: http://www.fda.gov/Safety/Recalls/ucm241602.htm.

Vargas AM, Kim MS, Tao Y, Lefcourt AM, Chen YR, Luo YG, Song YS & Buchanan R. 2005. Detection of fecal contamination on cantaloupes using hyperspectral fluorescence imagery. Journal of Food Science 70:E471-E476.

Wehry EL. 1990. Effects of Molecular Environment on Fluorescence and Phosphorescence. In: Guilbault, G. G., editor). Practical Fluorescence. Second ed. New York: Marcel Dekker, Inc. p. 127-184.

Wendel Arthur M, Hoang Johnson D, Sharapov U, Grant J, Archer John R, Monson T, Koschmann C & Davis Jeffrey P. 2009. Multistate outbreak of *Escherichia coli* O157:H7 infection associated with consumption of packaged spinach, August–September 2006: The Wisconsin Investigation. Clinical Infectious Diseases 48:1079-1086.

Whitehead KA, Smith LA & Verran J. 2008. The detection of food soils and cells on stainless steel using industrial methods: UV illumination and ATP bioluminescence. International Journal of Food Microbiology 127:121-128.

Xing J & De Baerdemaeker J. 2005. Bruise detection on 'Jonagold' apples using hyperspectral imaging. Postharvest Biology and Technology 37:152-162.